Research Square

Preprints are preliminary reports that have not undergone peer review.
They should not be considered conclusive, used to inform clinical practice,
or referenced by the media as validated information.

Aquaculture Expansion and Hydrometeorological Conditions in Brazil's Main Aquaculture Hub Using Machine Learning

Bruno Aparecido da Silva
Mixed Research and Innovation Unit (UMIPI) for West Paraná
Thomas Sponchiado Pastore
Biopark
Ericson Hideki Hayakawa
Western Paraná State University (UNIOESTE)
Altair Bennert
Western Paraná State University (UNIOESTE)
Marcos Adami
National Institute for Space Research
Débora Tatyane Oliveira Xavier
Mixed Research and Innovation Unit (UMIPI) for West Paraná
Marta Eichemberger Ummus
marta.ummus@embrapa.br

Brazilian Agricultural Research Corporation

Research Article

Keywords: sustainable, machine learning, water resources, climate change, aquaculture

Posted Date: June 11th, 2026

DOI: https://doi.org/10.21203/rs.3.rs-9838721/v1

License: This work is licensed under a Creative Commons Attribution 4.0 International License.
Read Full License

Additional Declarations: No competing interests reported.

Aquaculture Expansion and Hydrometeorological Conditions in Brazil's Main Aquaculture Hub Using Machine Learning

Abstract: Changes in land use and land cover in Brazil have reduced water availability, this scarcity affects pond-based aquaculture. In the face of hydrometeorological uncertainties in South America, this study analyzes the expansion of aquaculture and its relationship with water availability across river watersheds in the state of Paraná between 2015 and 2025, and projects precipitation scenarios through 2035. Sixteen river watersheds were evaluated using spatiotemporal data derived from remote sensing, geoprocessing, and a machine learning classifier implemented on the Google Earth Engine (GEE) platform. Furthermore, the Random Forest algorithm was employed to develop a predictive model of water availability for the state of Paraná. Temporal mapping achieved high overall accuracies, ranging from 0.89 to 0.98. The results indicate a spatially concentrated expansion of aquaculture farms in the Paraná and growth rates varying between 600% and 900%. Simultaneously, declining streamflow trends were observed across all analyzed watersheds. State-level aquaculture shows watersheds with water deficits and negative production correlations and favorable conditions and positive aquaculture growth, especially in western and northern regions of the state. Water availability prediction using Random Forest showed consistent average performance (R^2 = 0.73, MAE = 0.026, MSE = 0.001, and RMSE = 0.034). Analysis of precipitation projections (2026–2035) indicated a decreasing, particularly under the SSP2-4.5 scenario. This scenario presents a challenging outlook for aquaculture growth in the short to medium term, highlighting the need for continuous monitoring and geospatial planning to guide aquaculture expansion, promote a more balanced distribution of productivity, and enhance water security.

Keywords: sustainable; machine learning; water resources; climate change; aquaculture.

1. Introduction

By 2030, the global population is expected to reach 8.5 billion, and approximately 10 billion by 2050, intensifying pressure on food systems (FAO, 2024). This scenario makes the management of essential resources, such as water, even more critical, as water availability is expected to become increasingly scarce (Béné et al., 2015; Łągiewska & Bartold, 2025), particularly due to the impacts of climate change (Pérez-Cutillas & Salhi, 2024). In addition, changes in land use and land cover exert a direct influence on the functioning of river watersheds, affecting parameters such as water yield, surface runoff, and evapotranspiration (Kundu, Khare, & Mondal, 2017). These changes may lead to reduced water availability (Bao et al., 2019), as they contribute to decreased precipitation, rising temperatures, and intensified evapotranspiration (Ciampittiello, Marchetto, & Boggero, 2024; Novruzova, 2021). In this context, the adoption of planning and management actions becomes indispensable (Almeida et al., 2023; Guo et al., 2020).

Studies conducted in Brazil indicate that changes in land use and land cover have contributed to reduced precipitation and increased land surface temperature and evapotranspiration (Silva, Lopes, & Santos, 2023), directly affecting the water balance (Rocha et al., 2021) and water availability (Silva, Heriberto de Castro Teixeira, & Lilla Manzione, 2019). In recent years, southern Brazil has experienced significant losses in the agricultural sector, either due to severe droughts, such as those recorded in 2023, or floods, such as the events that occurred in May 2024 in the state of Rio Grande do Sul (Nóia-Júnior, Christo, & Pezzopane, 2025). Even in regions of the country with substantial water reserves, changes in basin hydrology have been observed, mainly associated with the expansion of monoculture systems (Cremon et al., 2025; Ferreira et al., 2023; Funatsu et al., 2025; Serrão et al., 2020). This set of changes is likely to significantly affect economic development, human livelihoods, and environmental quality (Nascimento, Borges, & Diniz

Melo, 2023) across several Brazilian regions (Tavares et al., 2023), with even more pronounced effects in productive sectors that depend on freshwater resources (Althoff, Rodrigues, & Silva, 2021; Rocha et al., 2021).

Trends in water availability in Brazil indicate a continuous increase in water consumption (ANA, 2024), in line with global trends (Siyal, Gerbens-Leenes, & Vaca-Jiménez, 2023). Although Brazil holds considerable water reserves (Barbedo et al., 2022), the emerging national water scenario is critical (Uchôa et al., 2024). According to the National Water and Sanitation Agency, the impacts of climate change are already being observed in national water resources, while water demand has increased substantially, with an estimated rise of approximately 80% in total water withdrawals over the past two decades (ANA, 2024). By 2030, demand is expected to increase by about 24%, mainly driven by the agricultural sector (Barbedo et al., 2022; Biazar et al., 2025; Greve et al., 2018; Mello et al., 2019; Passos et al., 2025).

In Brazil, aquaculture is often treated as a secondary activity, highlighting the need for a better understanding of its production chain (Valenti et al., 2021; Pacheco et al., 2025). Although it gained a more industrial profile in the 1970s (Loureiro et al., 2024; Valenti et al., 2021), the sector has since expanded to include over 60 edible species and around 250 ornamental species (Welter et al., 2021). Production increased from 476.5 thousand tons in 2013 to 791.5 thousand tons in 2023 (IBGE, 2024), with tilapia leading this growth and Paraná standing out as the main producer (Anuário Peixe BR, 2025; IBGE, 2024).

Given the impacts of climate change on aquaculture and food security (IPCC, 2023; WMO, 2023; FAO, 2020, 2024; Karanth et al., 2023), incorporating adaptation measures is essential, though limited by the lack of sector-specific analyses on vulnerabilities and risks (Naylor et al., 2021; Rajandran et al., 2022; Weitzman, Filgueira, & Grant, 2021; Barange et al., 2018). In Paraná, this requires short-term planning, improved water management, and investments in infrastructure and insurance (Vallino, Ridolfi, & Laio, 2020; Nóia-Júnior, Christo, & Pezzopane, 2025; Pillar & Overbeck, 2024). It also demands research and policies to guide aquaculture expansion under local conditions (Fong et al., 2024; Pacheco et al., 2025; Wrege et al., 2016; Novo et al., 2022). Adaptation depends on assessing future water demand and production risks, alongside sustainable water storage (Fong et al., 2024; Zhao et al., 2025b). While aquaculture supports food security, it may impact ecosystems (Wang et al., 2023), making geospatial tools essential for sustainable management and decision-making (São José et al., 2022; Wang et al., 2024; Dapieve et al., 2023; Ottinger et al., 2022).

Satellite remote sensing combined with geographic information systems has proven effective for complex analyses (Farias et al., 2023; Wang et al., 2024), including climate change impacts on water resources and assessments of water availability (Garajeh et al., 2024), especially in data-scarce regions (Laipelt et al., 2021). High-resolution aquaculture mapping supports inventory analyses and sustainable development (Ottinger, Clauss, & Kuenzer, 2018; Silva et al., 2024; Sun et al., 2024), as well as drought monitoring using precipitation and soil moisture data (AghaKouchak et al., 2015). Tools such as Google Earth Engine (GEE) expand these capabilities (Kumar & Mutanga, 2018; Vizzari et al., 2025) by enabling large-scale processing of remote sensing data (Amani et al., 2020; Campos-Taberner et al., 2018; Pérez-Cutillas et al., 2023; Velastegui-Montoya et al., 2023). These platforms support the monitoring of environmental dynamics and aquaculture expansion, as well as its relationship with water demand (Diniz et al., 2021; Silva et al., 2024; Souza et al., 2020), while contributing to ecosystem conservation (Amani et al., 2020; Silva et al., 2024; Sun et al., 2024). Integrated with artificial intelligence (Et-taibi et al., 2024; He et al., 2025), big data, and automation, they enhance the prediction of environmental scenarios (Erekalo et al., 2024), support climate adaptation strategies (Parra-López et al., 2025), and improve natural resource management through more efficient responses to water scarcity (Sapitang et al., 2024; Wang & Razmjooy, 2024).

Considering that aquaculture in Brazil has exhibited rapid growth compared to other major food production sectors (FAO, 2024), and that this production occurs predominantly in pond-based systems and cage culture, increasing pressure on water availability has been observed in river watersheds already affected by hydrometeorological events

(ANA, 2024). This context may compromise water availability for other uses (Laipelt et al., 2024) and pose challenges to water governance (Lopes et al., 2021; Yvoz et al., 2025), particularly in the process of granting water-use permits. Accordingly, this study investigates the expansion of aquaculture and its relationship with water availability in river watersheds between 2015 and 2025, including precipitation projections through 2035, in the state of Paraná, Brazil.

2. Methodology

2.1. Study Area

The study was conducted in the state of Paraná (Figure 1), southern Brazil, within the Atlantic Forest biome (Cunico & Prim, 2018). The climate is predominantly humid subtropical, with hot or mild summers (Alvares et al., 2013), and average annual precipitation is approximately 1,550 mm. The landscape is characterized by plateau surfaces with moderate to high drainage density and mostly flat to gently undulating relief, favoring agriculture. Deep soils (Ferralsols and Nitisols) dominate flatter areas, while shallow soils (Regosols, Leptosols, and Cambisols) occur in more dissected terrains (Silva et al., 2021).

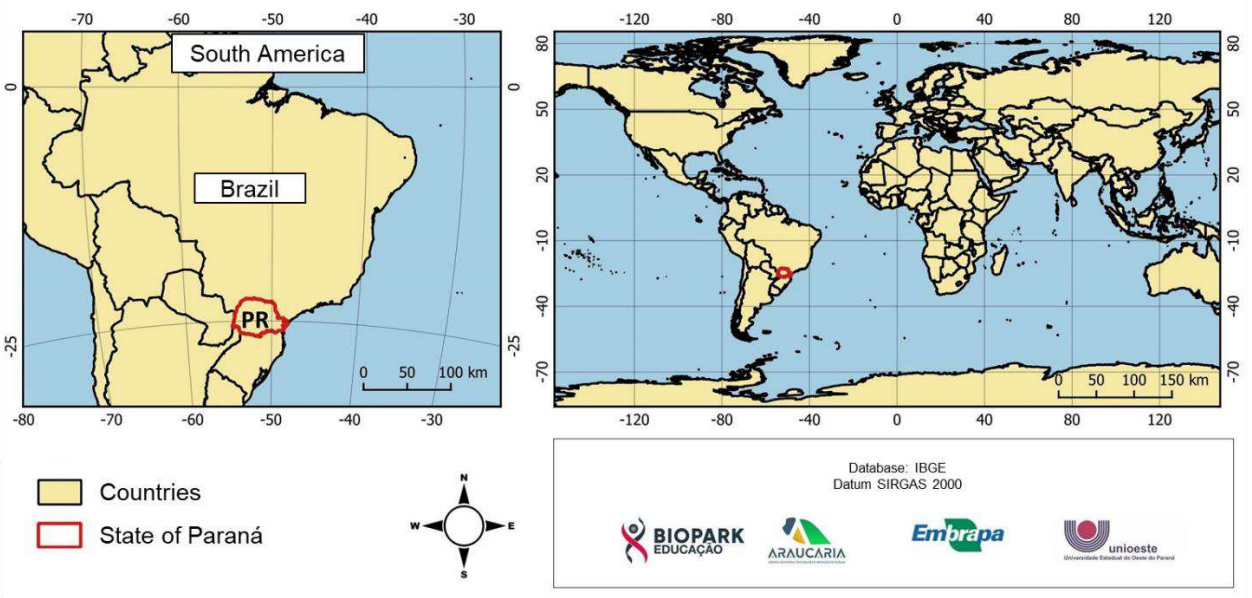


Figure 1. Location of the study area in Brazil.

2.2. Datasets

Aquaculture mapping used PlanetScope imagery (4.77 m resolution) (Planet Team, 2017), available via the Norway's International Climate and Forest Initiative (NICFI) program and accessed through Google Earth Engine (GEE) for 2015–2025. Hydroclimatic variables (2015–2024), including precipitation, evapotranspiration, temperature, runoff, soil moisture, and projections, were also obtained from GEE. Additional data on river discharge, basin boundaries, and aquaculture production were sourced from governmental databases (Table 1).

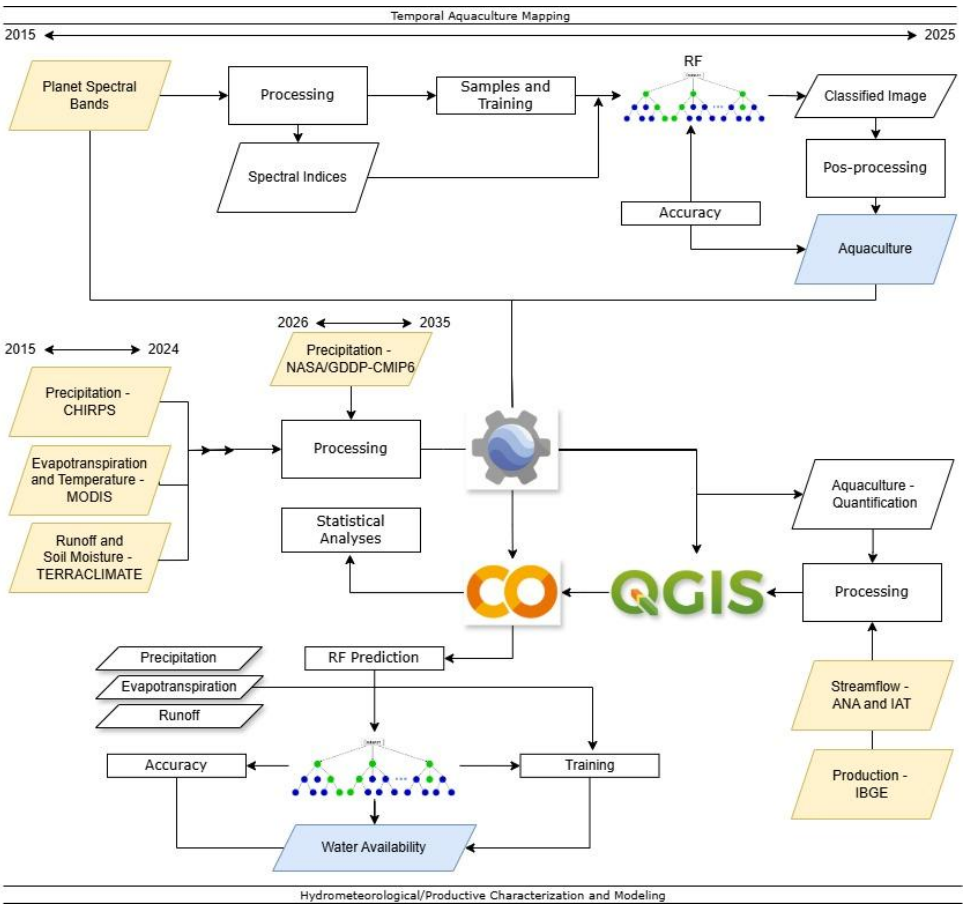


Figure 2. Methodological workflow.

2.3. Temporal Analysis of Aquaculture Farms.

Temporal mapping of aquaculture farms followed the methodology of Silva et al. (2024), based on pixel-oriented supervised classification of high-resolution PlanetScope imagery (4.77 m; B, G, R, and N bands) (Figure 2). Processing was carried out in the Google Earth Engine (GEE) platform (Gorelick et al., 2017), which enables large-scale data handling (Kanja et al., 2025). Spectral indices were extracted, and training and validation samples were collected to support classification into water and non-water classes, followed by post-classification refinement using geometric filters. Accuracy was assessed using the Random Forest (RF) algorithm, an ensemble method that reduces overfitting by combining multiple decision trees. For each pixel, the final class was defined by majority voting. Model performance was evaluated by reserving 20% of samples annually, generating confusion matrices (Figure 3c) and Overall Accuracy (OA) values (Table 2). Additionally, the spatial classification results were integrated into a Geographic Information System (GIS) environment (QGIS 3.28.2, 2024), where kernel density maps were produced.

Table 1. Summary of datasets used.

Variable	Source	Spatial Resolution	Temporal Resolution	Description	Reference
Spectral bands and indices	Imagens PlanetScope Norway's International Climate and Forest Initiative NICFI	4,77 m	Monthly	Provides monthly high-resolution satellite imagery to support tropical forest monitoring, emission reduction, and the prevention	PlanetScope, (2017)

Variable	Source	Spatial Resolution	Temporal Resolution	Description	Reference
				of deforestation and degradation.	
Precipitation (P, mm)	CHIRPS/DAILY (*Climate Hazards Group InfraRed Precipitation with Station Data*)	~5 km	Daily (monthly aggregated)	Combines satellite data and rain gauge observations; historical time series.	Funk et al. (2015)
Precipitation projections (P, mm)	NASA/GDDP-CMIP6 (*NASA Goddard Institute for Space Studies - Coupled Model Intercomparison Project Phase 6 - CMIP6*)	~27 km	Daily	Composed of downscaled global climate scenarios based on simulations, covering two greenhouse gas emission pathways known as Shared Socioeconomic Pathways (SSPs).	Tebaldi et al 2021
Actual evapotranspiration (ET, mm)	MODIS MOD16A2GF (*Moderate Resolution Imaging Spectroradiometer*)	500 m	8-day (monthly aggregated)	Estimates based on ecophysiological and meteorological algorithms; suitable for hydrological monitoring.	NASA (2023)
Surface runoff (RO, mm)	TerraClimate	~4 km	Monthly	Data derived from meteorological observations and reanalysis; consistent at the regional scale.	Abatzoglou et al. (2018)
Soil moisture (SM, mm)	TerraClimate	~4 km	Monthly	Estimates based on simplified hydrological models and climatic water balance.	Abatzoglou et al. (2018)
Land surface temperature (LST, °C)	MODIS MOD11A2	1 km	8-day (monthly aggregated)	Provides Land Surface Temperature (LST); converted to °C using a scale factor (0.02) and Kelvin–Celsius adjustment.	NASA (2023)
River discharge ($m^3 s^{-1}$)	Streamflow gauge data – National Water and Basic Sanitation Agency (ANA); Water and Land Institute of the State of Paraná (IAT)	Point-based	Daily		ANA (2025); IAT (2025)
Production (R$ and kg)	Gross Production Value – Brazilian Institute of Geography and Statistics (IBGE)	National	Annual	Open data portal providing public access to water resources data and information for Brazil and the state of Paraná.	IBGE (2024)
Administrative and basin boundaries	Sixteen river watersheds from the Water and Land Institute of the State of Paraná (IAT)	State-level	-		IAT (2025)

2.4. Temporal Analysis of Hydrometeorological Variables

Hydrometeorological data (precipitation, evapotranspiration, runoff, and land surface temperature) were processed in Google Earth Engine (GEE) using scripts for variable extraction and precipitation projections (Dahan et al., 2023; Zhao, Lu, & Wei, 2019). The 16 watersheds of Paraná were imported as a FeatureCollection, enabling spatial clipping and time series generation (2015–2024), with precipitation derived from CHIRPS. Evapotranspiration was obtained from MODIS (MOD16A2GF), runoff from TerraClimate, and soil moisture from MODIS, supporting water availability and drought/flood assessments (Chernykh et al., 2025). Land surface temperature was derived from MODIS (MOD11A2) (Ji et al., 2025; Tanuja & Kumar, 2025). Precipitation projections were based on the ACCESS-ESM1-5

model (CMIP6/NASA-GDDP) (Thrasher et al., 2022), which performs well in South America (Tebaldi et al., 2021), considering SSP2-4.5 and SSP5-8.5 for 2026–2035. Data were aggregated into monthly time series using ee.Reducer.mean, and water availability was estimated through a balance between inputs and outputs (Amiri, Salem, & Ghzal, 2022).

Statistical analyses were conducted in Google Colab, applying Mann-Kendall and Theil-Sen tests to identify trends (Battisti et al., 2025). Streamflow gaps from ANA stations were filled using a Random Forest Regressor, though Paranapanema I and II were excluded due to data unavailability.

2.5. Time-Series Analysis of Aquaculture Production

Aquaculture production data (quantity in kg and value in R$) for 2014–2024, obtained from Brazilian Institute of Geography and Statistics (IBGE), were organized into annual time series and analyzed to detect spatio-temporal trends, following the same procedures applied to environmental variables. Interannual (YoY) variations were calculated as percentage growth or decline for each watershed (Table 2; Eqs. 2 and 3), enabling the identification of short-term dynamics. Analyses and visualizations (time series, scatter plots, and boxplots) were developed in Google Colab to represent YoY distributions across watersheds.

2.6. Correlation and Clustering Analyses

Correlation analyses make it possible to identify which variables exert the greatest influence on the variability of others, representing a fundamental step for decision-making in agriculture and natural resource management (Melnyk & Brunn, 2025). To this end, the Pearson correlation coefficient was applied to quantify the strength and direction of linear relationships between environmental (hydrometeorological) and production variables (Yu et al., 2025). In parallel, Principal Component Analysis (PCA) was employed, a technique that enables the identification of the components responsible for explaining most of the observed variance in the dataset (Melnyk & Brunn, 2025).

$$\text{Total Growth Rate (\%)} = \left(\left((Vfinal - Vinitial)/Vinitial\right)\text{^}\right) = e$$

Table 2 – Metrics used to evaluate the performance of the RF algorithm, mapping, and model.

Metric	Description	Eqution	
Water Availability	DH - Water Availability; P - Precipitation; ET - Evapotranspiration; RO - SurfaceRunoff.	DH = P – (ET + RO)	eq. 1
Total Growth Rate	V_{final} - Final value; $V_{initial}$ - Initial value	Total Growth Rate (%) = $((Vfinal - Vinitial)/Vinitial)\times 100$	eq.2
Year-over-Year (YoY) Growth Rate	V_t - Value in the current year; V_{t-1} - Value in the previous year.	YoY (%) = $((Vt - Vt - 1)/(Vt - 1))\times 100$	eq.3

Overall Accuracy	x_{ii} - number of correctly classified samples for class i; n - total number of classes; N - total number of samples.	$OA = \frac{\Sigma_{i=1}^{n} x_{ii}}{N}$	eq. 4
R^2	The Coefficient of Determination (R^2) measures how well the model fits the data, ranging from 0 (poor fit) to 1 (perfect fit). n - number of observations	$R2 = 1 - \frac{\Sigma_{i=1}^{n} (predicted_i - actual_i)^2}{\Sigma_{i=1}^{n} (actual_i - mean(actual))^2}$	eq. 5
Mean Squared Error (MSE)	Measures the average of the squared differences between predicted and observed values, indicating the overall quality of the predictions; lower values represent higher model accuracy.	$MSE = \frac{1}{n}\sum_{i=1}^{n} (predicted_i - actual_i)^2$	eq.6
Root Mean Squared Error (RMSE)	Indicates the average prediction error in the original units of measurement, obtained by taking the square root of the MSE; lower values represent higher model accuracy.	$RMSE = \sqrt{\frac{1}{n}\sum_{i=1}^{n} (predicted_i - actual_i)^2}$	eq.7
Mean Absolute Error (MAE)	measures the average of the absolute differences between predicted and observed values, providing a direct measure of the magnitude of prediction errors. Lower values indicate higher model accuracy.	$MAE = \frac{1}{n}\sum_{i=1}^{n} \lvert predicted_i - actual_i \rvert$	eq.8

2.7. Prediction of Water Availability

With the aim of contributing to the understanding of future environmental scenarios (Erekalo et al., 2024) that may affect the expansion of fish farming, a machine learning based model was developed to predict water availability (Sapitang et al., 2024; Wang & Razmjooy, 2024; Gao et al., 2025).

Data processing and modeling were conducted in Python 3.x using libraries such as pandas and numpy (data manipulation), matplotlib (visualization), scipy (statistics), scikit-learn (modeling and metrics), statsmodels (STL decomposition), and optuna (hyperparameter optimization). Precipitation, evapotranspiration, surface runoff, and water availability data were organized into watershed time series and normalized to a 0 - 1 range using MinMaxScaler (Pedregosa et al., 2011). This step was necessary to address differences in data scale and avoid imbalanced weighting in the model (Han et al., 2011).

For each watershed, the predictor variables were selected, and the dataset was divided into two subsets: one containing environmental parameters (predictor variables) and the other containing the resulting water availability. These datasets were further subdivided by watershed, generating 16 independent datasets. To reduce the influence of seasonality without altering the overall trend of the series, Seasonal and Trend decomposition using Loess (STL) was applied to attenuate variations extrinsic to the analyzed parameters (Cleveland et al., 1990; Hyndman & Athanasopoulos, 2018). This step enables the model to learn the true effects of the parameters without interference from large interannual fluctuations, such as those associated with El Niño and La Niña events, which frequently modulate water availability at continental scales.

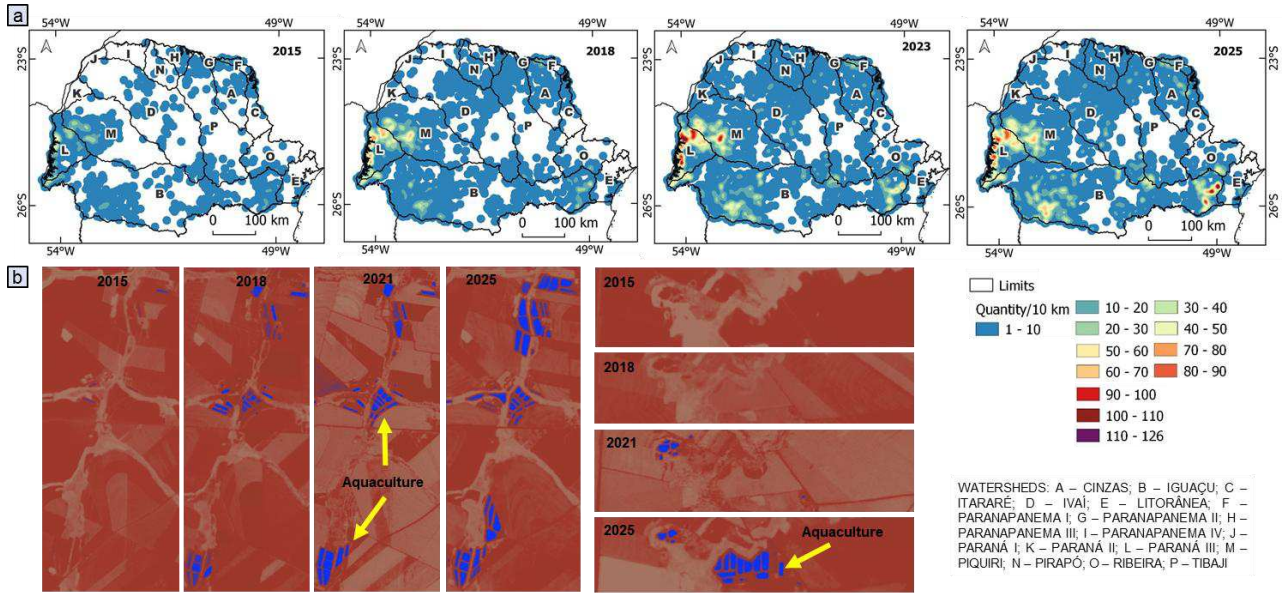
The predictive model adopted was the Random Forest (RF) algorithm (Breiman, 2001), due to its robustness, ability to handle high-dimensional data (Mohammadi et al., 2025), and excellent performance in environmental studies (He et al., 2025). To maximize model performance, the main hyperparameters (n_estimators, max_depth, min_samples_split, min_samples_leaf) were optimized using the Optuna framework, with the objective function defined as the maximization of the mean coefficient of determination (R^2) obtained from cross-validation splits (Akiba et al., 2019; Bergmeir et al., 2017; Gupta et al., 2009).

After signal filtering and watershed-based organization, the data were divided into two periods: data prior to January 2023 were used for model training, while data from January 2023 onward were reserved for model testing. Each training subset corresponding to a watershed was submitted to the Optuna framework (Akiba et al., 2019) using a five-fold time-based split, in which each segment was used for training and the subsequent segment for validation (Bergmeir et al., 2017), resulting in an independent model for each watershed (Gupta et al., 2009). With the optimized hyperparameters, the model was trained using the training dataset and subsequently applied to predict water availability for the period from 2023 to 2024 for each watershed, followed by performance evaluation of the model (Table 2).

3. Results

3.1. Spatial and Temporal Analysis of Aquaculture

With accuracy ranging from 0.89 (2015) to 0.97 (2025), the RF classifier enabled the identification of a pronounced spatial expansion of areas allocated to aquaculture production in excavated ponds in the state of Paraná (Figures 3; 4a, d). The spatiotemporal mapping (Figure 3a) revealed a relatively low spatial concentration of aquaculture across the state, with a predominance of 1 to 10 aquaculture farms within a 10 km radius in most hydrographic watersheds. The highest concentrations were observed in the Paraná III and Piquiri watersheds, where densities ranging from 1 to 50 aquaculture farms per 10 km were recorded. In 2015, the total aquaculture area in the state was less than 5,000 ha, encompassing approximately 3,000 aquaculture farms (Figure 4a), and fish production was below 75,000 kg, corresponding to a market value of approximately R$ 0.4 billion.



c

Year	2015		2016		2017		2018		2019		2020		2021		2022		2023		2024		2025	
	N	A	N	A	N	A	N	A	N	A	N	A	N	A	N	A	N	A	N	A	N	A
N	271	19	163	5	163	5	162	6	156	12	161	7	163	5	284	6	163	5	162	6	165	3
A	22	62	4	56	5	65	11	59	10	60	4	66	4	66	2	68	10	60	9	61	5	65
AO	0,89		0,96		0,96		0,93		0,91		0,95		0,96		0,98		0,94		0,94		0,97	

Figure 3 – Spatiotemporal evolution of aquaculture expansion in excavated ponds in Paraná (a, b) and overall accuracy (c).

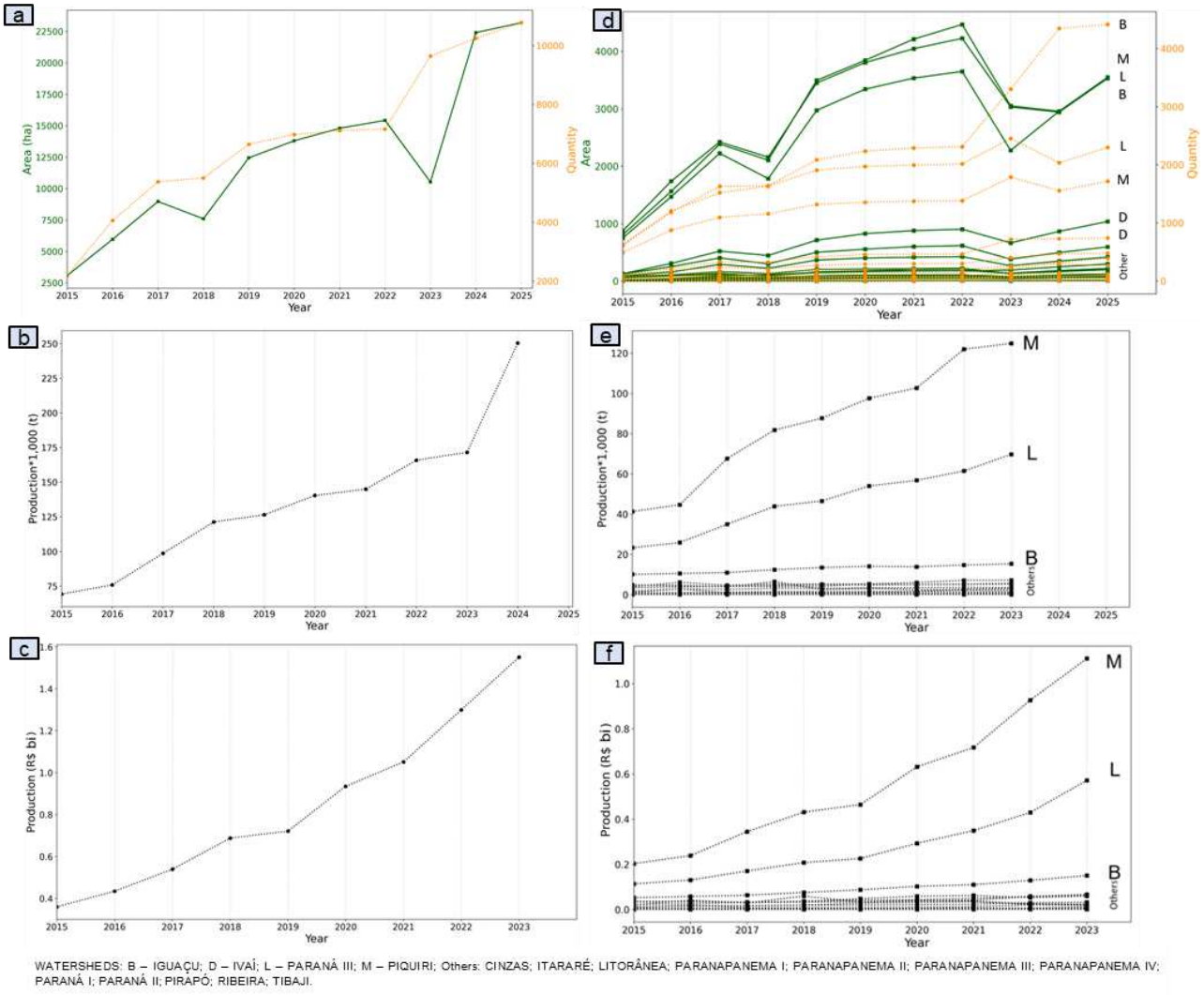


Figure 4 – Analysis of the evolution of aquaculture area and production in Paraná (a, b, c) and by hydrographic basin (d, e, f).

From 2018 onward, a marked increase in the number of aquaculture farms was observed (Figure 4d) in the Paraná III, Piquiri, and Iguaçu watersheds, resulting in a higher incidence of areas with enterprise densities ranging from 50 to 80 aquaculture farms per 10 km. This expansion was consolidated in 2023, when the Paraná III and Piquiri watersheds began to exhibit aquaculture hotspots, reaching up to 126 aquaculture farms within a 10 km radius. Spatial expansion was also observed in the Iguaçu basin, accompanied by increased clustering, reaching 80 to 90 aquaculture farms per 10 km. Despite this overall expansion, two periods of contraction in the total area occupied by aquaculture farms were identified (Figure 4a). In 2017, the area decreased from approximately 9,000 ha to about 7,500 ha, while in 2022 a reduction from 15,000 ha to approximately 9,500 ha was recorded. Nevertheless, production values maintained an upward trajectory, particularly in the Paraná III and Piquiri watersheds. In the remaining watersheds, stagnation was observed in both production volume and value, with the exception of the Iguaçu basin, which showed a slight increase in production value (R$) (Figure 4b, c, e, f).

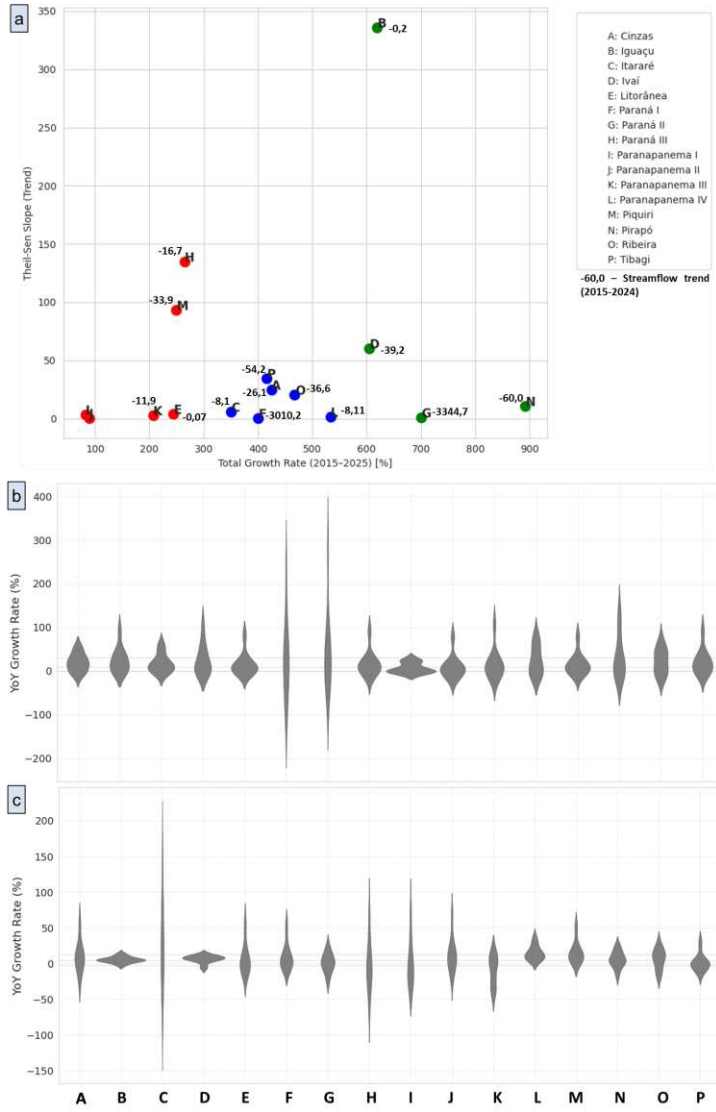
Table 3 – Assessment of streamflow trends and total percentage growth in production.

Watershed	Slope m^3s month	p value	Total Trend Streamflow m^3s	Total Growth Production% (kg)
Cinzas	-0,2198	0	-26,16	82,04
Iguaçu	-0,0022	0,001	-0,26	51,62
Itararé	-0,0681	0	-8,11	156,08
Ivaí	-0,3297	0,0166	-39,23	62,44
Litorânea	-0,0006	0,8685	-0,07	45,92
Paranapanema I	-	-	-	-16,92
Paranapanema II	-	-	-	124,87
Paranapanema III	-0,0932	0	-11,09	-62,28
Paranapanema IV	-0,0682	0	-8,11	198,58
Paraná I	-25,2966	0	-3010,29	89,96
Paraná II	-28,1073	0	-3344,77	0,48
Paraná III	-0,1359	0,0002	-16,17	-53,06
Piquiri	-0,285	0,0799	-33,92	202,23
Pirapó	-0,5046	0	-60,05	49,55
Ribeira	-0,3078	0	-36,63	52,15
Tibagi	-0,4556	0,0006	-54,21	8,25

In 2025, the Iguaçu, Paraná III, and Piquiri watersheds reached the highest concentrations of aquaculture farms, with values ranging from 100 to 126 aquaculture farms per 10 km. These watersheds also exhibited the highest values of area and number of aquaculture farms (Figure 4d), with the Iguaçu basin accounting for approximately 4,000 aquaculture farms. In addition, localized hotspot formations were identified in the Cinzas, Ivaí, Paranapanema I, and Tibagi watersheds (40 to 60 aquaculture farms per 10 km). The remaining watersheds maintained areas smaller than 1,000 ha and approximately 1,000 aquaculture farms (Figure 5d). The main producing watersheds, Piquiri and Paraná III, recorded approximately 160 thousand tons of production and a production value of R$ 1.4 billion in 2023. With a smaller contribution, the Iguaçu basin presented production below 20,000 t and approximately R$ 0.1 billion, while the other watersheds exhibited residual production levels (<10 thousand t; R$ 0.1 billion each). Overall, the analysis indicates consistent growth throughout the study period, reaching approximately 250 thousand t in 2024, and totaling about 11,000 aquaculture farms and 22,500 ha of occupied area statewide by 2025 (Figure 4a, b).

Regarding the relationship between the growth of the area occupied by aquaculture farms (2015–2025) and streamflow trends in the studied watersheds (Figure 5a; Table 3), only the Coastal basin exhibited hydrological stability (-0.07 $m^3\ s^{-1}\ yr^{-1}$) while simultaneously showing aquaculture growth close to 200%. Among all analyzed watersheds, the Pirapó, Paraná II, and Ivaí watersheds recorded the highest growth rates in aquaculture farms (Figure 4a), ranging from 600% to 900%. However, these watersheds also exhibited pronounced negative streamflow trends, varying from -39 to -3,444.7 $m^3\ s^{-1}\ yr^{-1}$. Although the Iguaçu basin showed substantial growth over the analyzed period (600%), the decreasing streamflow remained low throughout the time series (-0.2 $m^3\ s^{-1}\ yr^{-1}$). The Cinzas, Itararé, Paraná I, Paranapanema IV, Ribeira, and Tibagi watersheds exhibited growth rates between 350% and 550%, with predominantly negative streamflow trends ranging from -8.1 to -3,020.2 $m^3\ s^{-1}\ yr^{-1}$. The remaining watersheds showed growth below 300%, with streamflow trends ranging from -11.9 to -33.9 $m^3\ s^{-1}\ yr^{-1}$. Notably, in watersheds where fish farming has become consolidated in

recent years (Paraná III and Piquiri), growth was approximately 250%, also accompanied by negative streamflow trends (-16.7 to -33.9 $m^3 s^{-1} yr^{-1}$).



d

Watersheds	Year	Area	Quantity
Cinzas	2015	94,0	74
Cinzas	2025	417,2	388
Iguaçu	2015	750,4	613
Iguaçu	2025	3548,7	4412
Itararé	2015	20,4	20
Itararé	2025	83,6	90
Ivaí	2015	128,1	105
Ivaí	2025	1037,6	740
Litorânea	2015	74,4	25
Litorânea	2025	297,5	86
Paraná I	2015	6,6	5
Paraná I	2025	6,6	5
Paraná II	2015	0	0
Paraná II	2025	14,4	8
Paraná III	2015	874,2	631
Paraná III	2025	3529,2	2299
Paranapanema I	2015	86,5	50
Paranapanema I	2025	204,5	91
Paranapanema II	2015	21,9	9
Paranapanema II	2025	115,9	17
Paranapanema III	2015	19,5	15
Paranapanema III	2025	125,8	46
Paranapanema IV	2015	10,9	3
Paranapanema IV	2025	65,9	19
Piquiri	2015	805,5	491
Piquiri	2025	3547,3	1715
Pirapó	2015	14,4	12
Pirapó	2025	219,2	119
Ribeira	2015	55,3	46
Ribeira	2025	197,3	261
Tibagi	2015	122,0	93
Tibagi	2025	595,3	480
Total	**2015**	**3084,1**	**2192**
	2025	**14006,1**	**10776**

Figure 5 – Analysis of the growth rate of productive aquaculture area and streamflow by hydrographic basin. (b) number of aquaculture farms; (c) production (kg); (d) synthesis of aquaculture expansion, including initial and final conditions, area, and number of aquaculture farms.

An analysis of Figure 5b indicates that the Paraná I, Paraná II, and Pirapó watersheds exhibited the greatest amplitude of variation in the annual growth rate of the number of aquaculture farms, with oscillations that included periods of expansion approaching 400% and phases of spatial contraction reaching -200%. The Paranapanema I basin showed the lowest variability, with enterprise growth rates ranging between -10% and 50%. Regarding the annual variation in production (kg), more pronounced values were observed in the Itararé, Paraná III, and Paranapanema I and II watersheds (Figure 5c), which recorded increases between 100% and 250%, as well as sharp declines in production, ranging from -50% to -150%. For most watersheds, annual production growth rates remained within a narrower interval, between 0% and 20% (Table 3).

3.2. Hydrometeorological Analysis

The hydrometeorological analysis revealed that all watersheds exhibited a decreasing trend in precipitation throughout the historical time series. Specifically, the Iguaçu, Ivaí, Paraná I, II, and III, Paranapanema I, II, III, and IV, Piquiri, Pirapó, and Tibagi watersheds recorded periods with high monthly precipitation totals, reaching up to 566.93 mm, with a mean of 119.60 mm month^{-1}. The highest mean precipitation observed in the study area was 120.60 mm month^{-1}, recorded in the Coastal basin, which also exhibited the highest evapotranspiration (166.22 mm) and surface runoff values (248.23 to 317.57 mm) (Figures 6 and 7).

Overall, evapotranspiration values remained close to 153.0 mm month^{-1}, particularly in the Ivaí, Piquiri, and Paraná II watersheds, while mean surface runoff was approximately 29.95 mm month^{-1}. Soil moisture ranged from 3.03 to 59.77 mm, and land surface temperature varied between 8.36 and 25.03 °C in the Iguaçu, Ivaí, Paraná I, II, and III, Paranapanema I, II, III, and IV, Piquiri, Pirapó, and Tibagi watersheds. Land surface temperature exhibited an increasing trend over the analyzed period, ranging from 0.03 to 0.09 °C yr^{-1} (Figure 6). In the remaining watersheds Cinzas, Itararé, Coastal, and Ribeira soil moisture values remained below 76.77 mm throughout the time series (Figure 6).

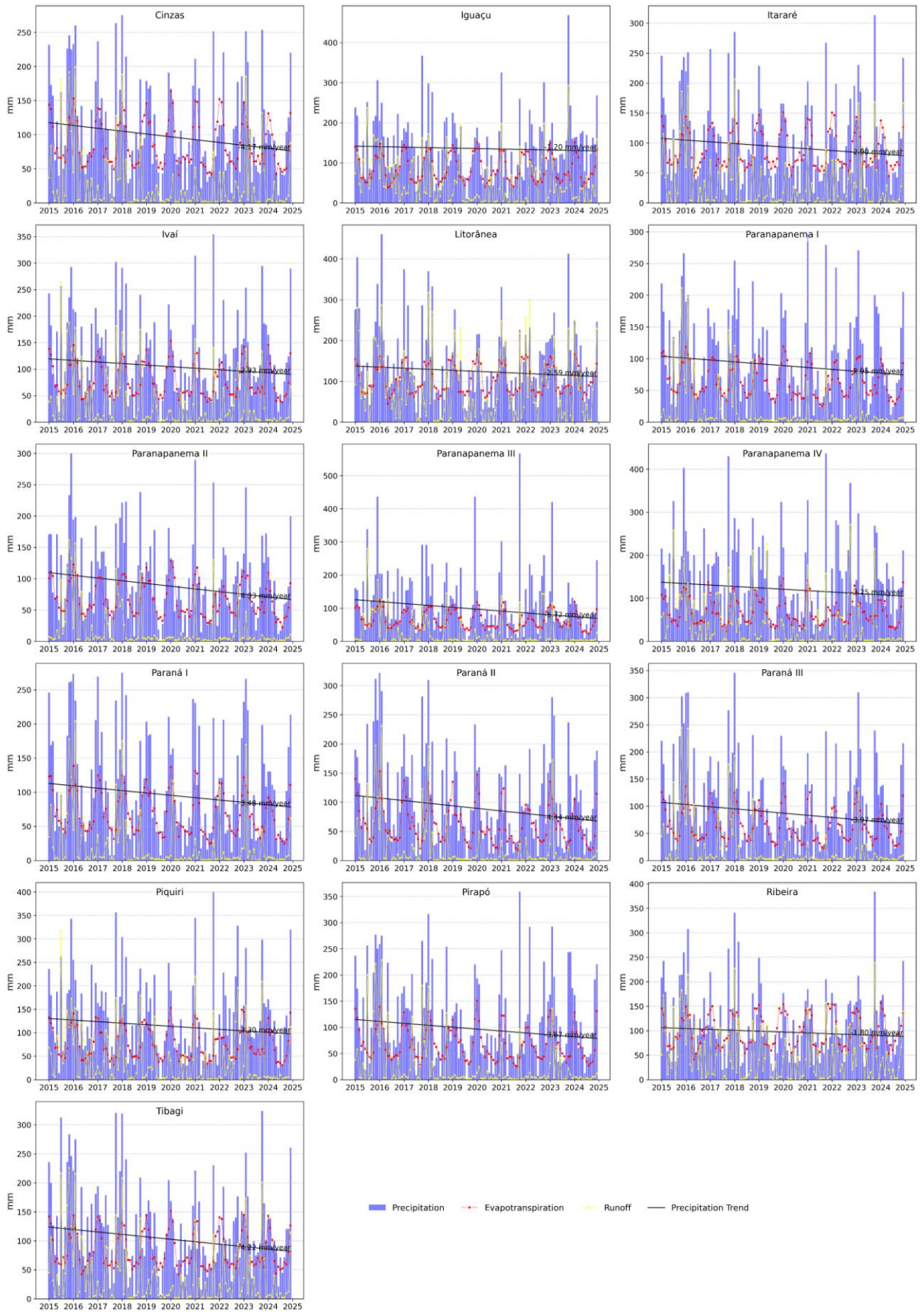


Figure 6 – Time series of hydrometeorological variables in the hydrographic watersheds of Paraná, 2015–2024.

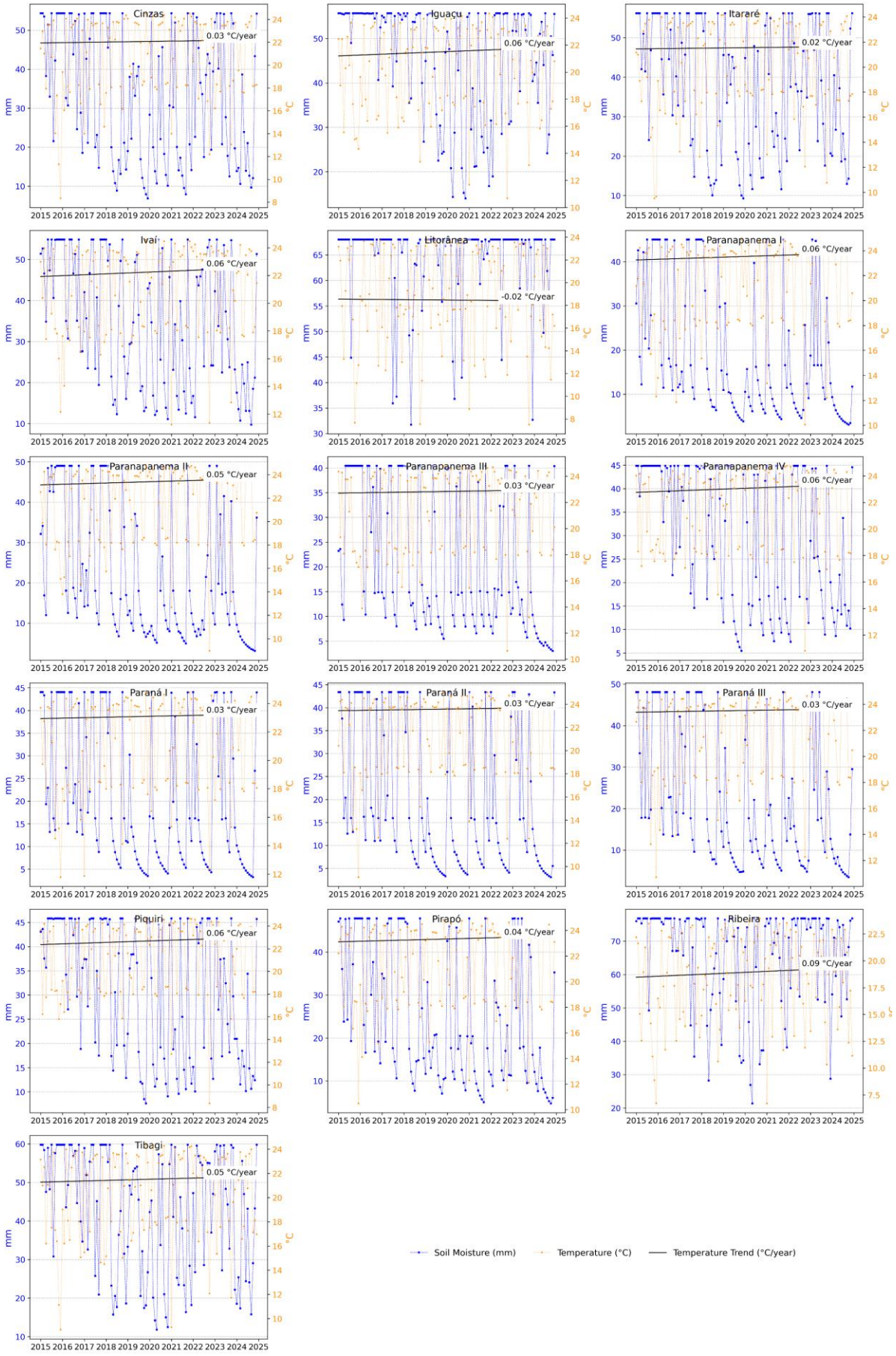


Figure 7 – Time series of hydrometeorological variables in the hydrographic watersheds of Paraná, 2015–2024.

3.3. Clustering and Correlation

With 70.3% of the variance explained, the cluster analysis separated the watersheds into three groups. Cluster 1 includes the majority of the hydrographic watersheds Cinzas, Itararé, Ivaí, Paranapanema I, II, III, IV, Paraná I, II, Pirapó, Ribeira, and Tibagi mainly distributed in the negative quadrant of PC1, associated with streamflow and evapotranspiration variables. In the positive quadrant, despite lower land surface temperature and streamflow, soil moisture, evapotranspiration, water availability, and surface runoff are linked to these watersheds. Cluster 2 (Coastal basin) is positioned in the negative PC1 and positive PC2 space, also related to soil moisture and evapotranspiration variables, but distinguished by a lower influence of water availability. Cluster 3 predominantly occupies the positive PC1 quadrant, with the watersheds in this cluster Iguaçu, Piquiri, and Paraná III associated with aquaculture production, encompassing higher values of productive area, production quantity, and production value.

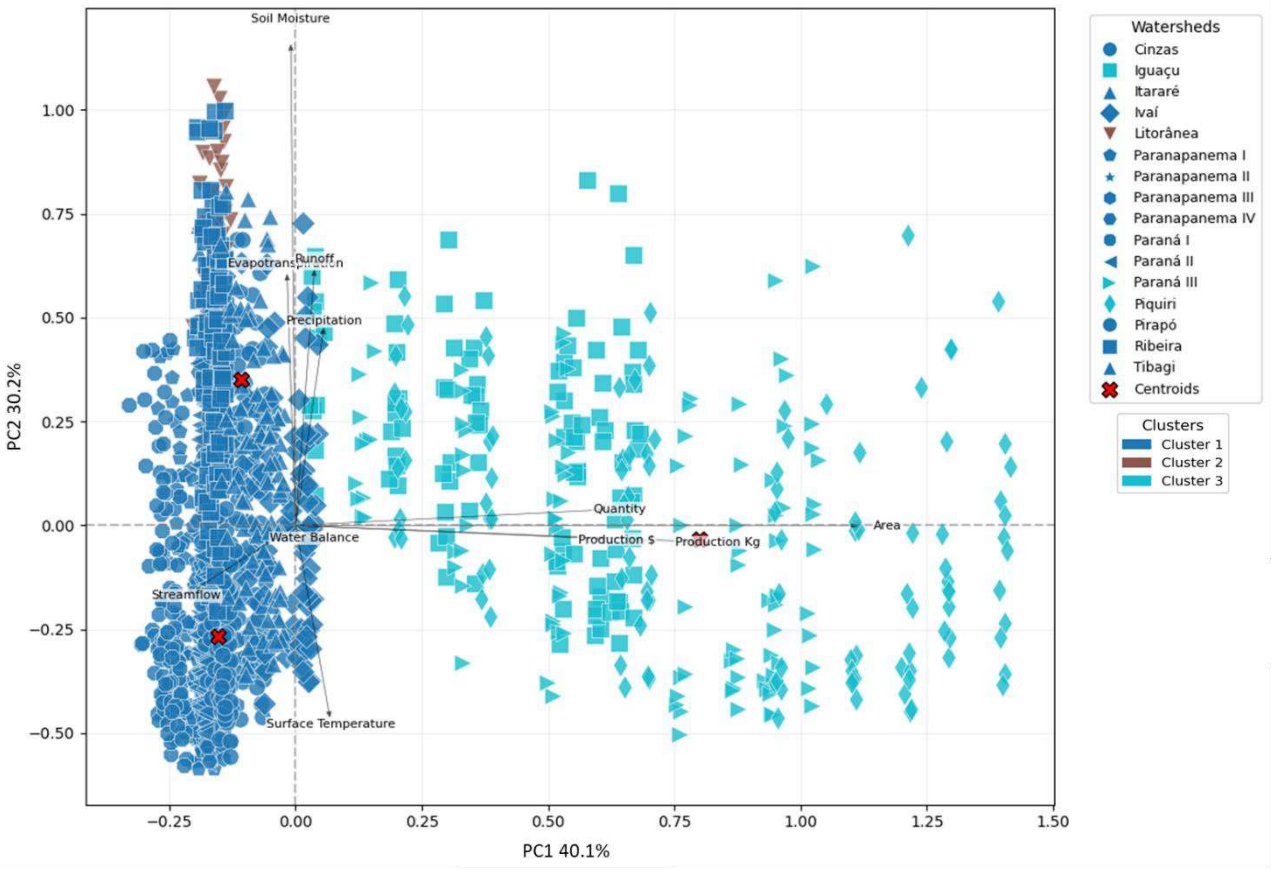


Figure 8 – Multivariate analysis of hydrometeorological variables and aquaculture production in the watershed of Paraná.

Pearson correlation analysis (Figure 9) revealed distinct patterns, as detailed below. Water availability showed predominantly positive correlations, particularly in the Iguaçu, Ivaí, Paraná I, III, and Piquiri watersheds, with coefficients reaching 0.63, except for evapotranspiration, surface runoff, and temperature, which exhibited negative correlations. Evapotranspiration, in turn, correlated negatively with production-related variables, with coefficients up to -0.19. Precipitation showed coefficients close to 0.82, primarily with water availability, evapotranspiration, soil moisture, and streamflow. Surface runoff was negatively correlated with production variables and positively correlated with soil moisture and streamflow, a pattern similarly observed for soil moisture and streamflow themselves. The variables number of aquaculture farms, occupied area, production (kg), and production value (R$) showed correlations above 0.90 among themselves and with time (year), reinforcing a trend of territorial expansion, particularly in the Cinzas, Iguaçu, Itararé,

Ivaí, Paranapanema IV, Piquiri, Pirapó, Ribeira, and Tibagi watersheds, and to a lesser extent in Paraná III. However, in the Paranapanema III, IV, and Paraná II watersheds, despite the positive correlation between the number of aquaculture farms and time, no strong correlation was observed for production in kg or R$, suggesting that physical expansion of aquaculture activities does not proportionally translate into higher productivity.

3.4. Water Availability, Prediction, and Future Precipitation

The Litorânea, Ribeira, Cinzas, and Itararé watersheds exhibited the highest frequency of periods with water deficits (Figure 10a), with values ranging from -206.09 mm to 112.84 mm and a mean value of -22.72 mm. The Litorânea and Itararé watersheds showed negative trends, ranging from 0.001 to -1.69 mm yr^{-1}, whereas the Ribeira and Cinzas watersheds exhibited increasing trends, with values between 0.23 and 0.70 mm yr^{-1}.

The remaining watersheds—Iguaçu, Ivaí, Paraná I, II, III, Paranapanema I, II, III, IV, Piquiri, Pirapó, and Tibagi displayed a higher frequency of positive water availability values (Figure 10a) and recorded positive trends in water availability, ranging from 0.08 to 4.67 mm yr^{-1}. The analysis also indicated that the Ivaí, Iguaçu, and Piquiri watersheds experienced successive periods of water deficit, particularly between 2015 and 2018. The largest water deficits were observed in the Paraná III and Piquiri watersheds, with values of -122.18 mm and -109.14 mm, respectively, while the highest water availability was recorded in the Paraná II basin, reaching 396.54 mm.

Considering the trend analysis of water availability (Figure 10b), the Litorânea basin exhibited a reduction of -16.90 mm between 2015 and 2024. The Itararé, Paraná II, Cinzas, Tibagi, Paranapanema II, and Ribeira watersheds accumulated between 0.0 and 10.0 mm, while the remaining watersheds showed accumulated values between 10.1 and 46.7 mm.

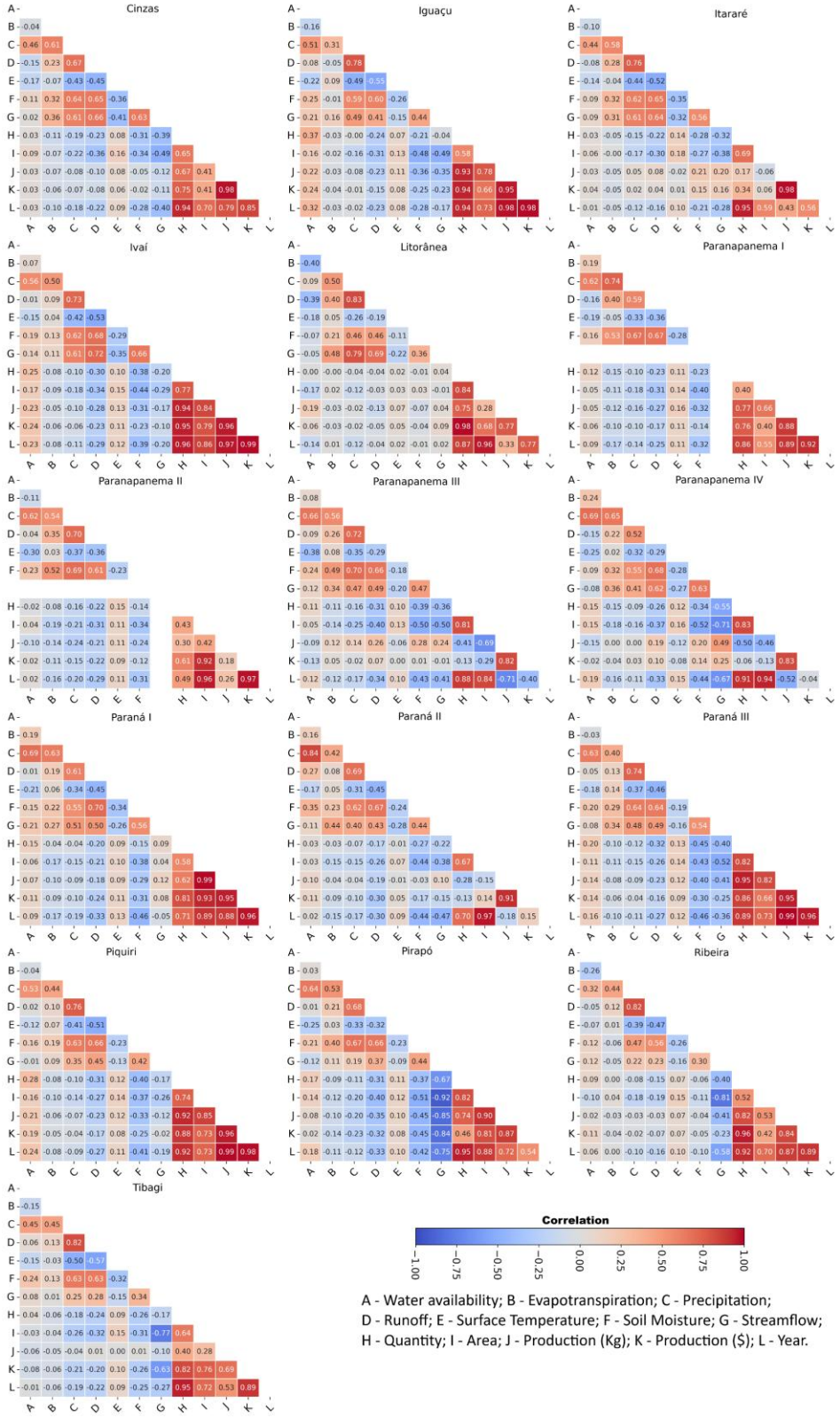


Figure 9 – Statistical correlation between hydrometeorological variables and aquaculture production in the watersheds of Paraná.

The average water availability of the studied watersheds (Figure 11b) revealed marked spatial heterogeneity. Watersheds located in the western sector of the state (Paraná I and II) exhibited the highest annual mean water availability, ranging from 30.14 to 32.42 mm. In the northern and northeastern regions (Paranapanema I, II, III, and Pirapó), mean values ranged from 14.06 to 26.96 mm. The Piquiri, Iguaçu, Ivaí, and Tibagi watersheds showed annual mean values

between 0.41 and 14.94 mm, while the remaining watersheds had the lowest annual means (-3.51 to -43.12 mm), indicating more critical conditions in the northeastern and eastern sectors.

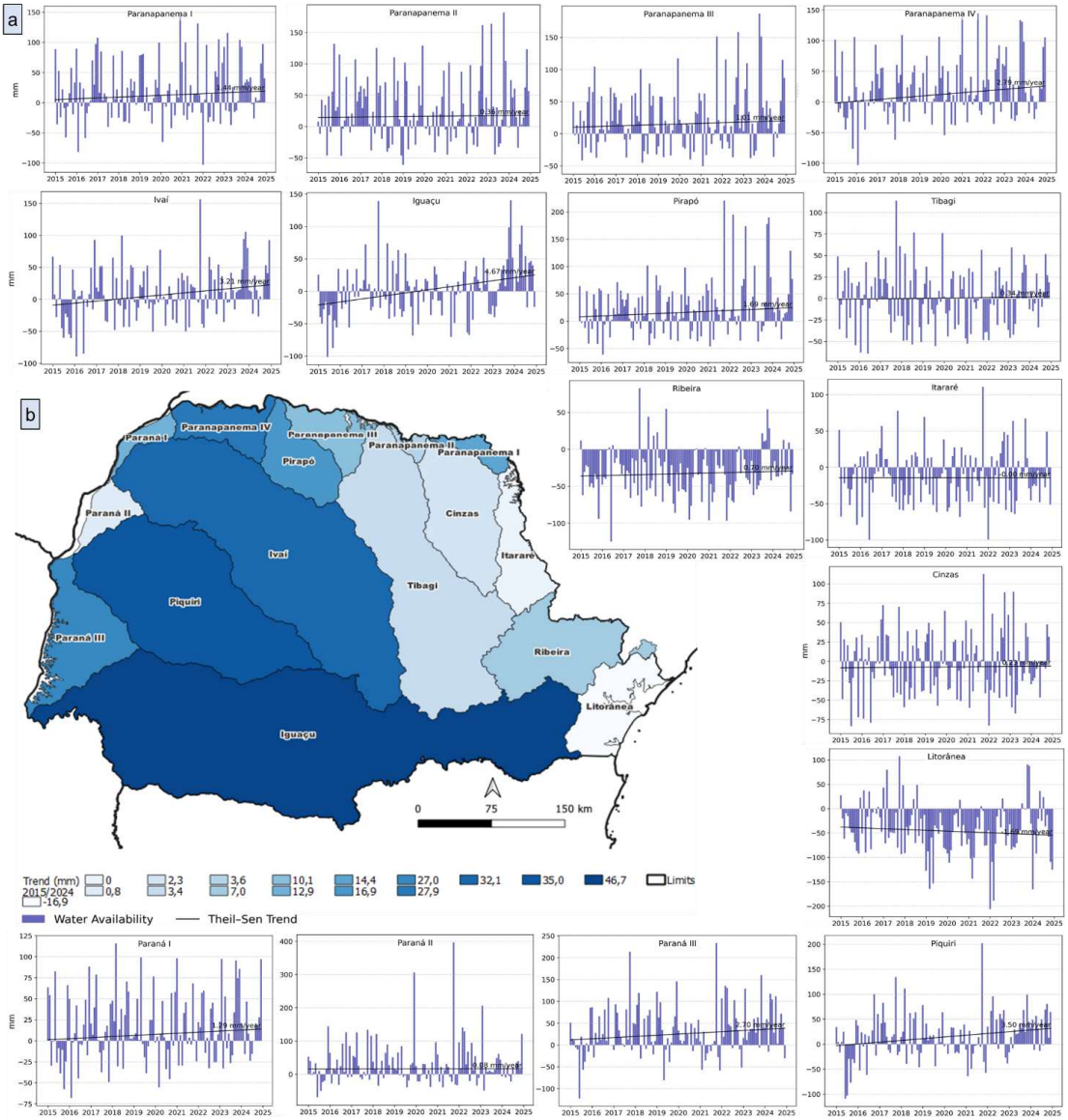


Figure 10 – Time series (a) and trend of water availability by hydrographic basin (b) in Paraná.

The prediction of water availability using machine learning (RF) showed better performance in the Paraná II and Paranapanema II watersheds, both with R^2 values above 0.8. In contrast, the Ribeira, Tibagi, Iguaçu, and Itararé watersheds exhibited more modest performance, with R^2 values below 0.6. The model effectively captured the interannual variability of water availability and demonstrated a stronger fit to the observed values, particularly in the watersheds located in the western, northwestern, and northern sectors. In these regions, R^2 values were predominantly above 0.70, covering nine of the sixteen watersheds analyzed (Table 4).

Table 4 – Evaluation of RF model performance and trends in precipitation projections.

Watershed	Acuracy RF				Projections – 2026-2030			
	R^2	MAE	MSE	RMSE	SSP2-4.5 – Slope mm/month	SSP2-4.5 p value	SSP5-8.5 Slope mm/month	SSP5-8.5 p value

Cinzas	0,827	0,017	0,001	0,025	-0,024	0,857	-0,070	0,883
Iguaçu	0,462	0,037	0,002	0,045	-0,025	0,764	0,054	0,434
Itararé	0,579	0,028	0,001	0,038	-0,007	0,913	-0,060	0,979
Ivaí	0,675	0,025	0,001	0,034	-0,007	0,877	-0,050	0,704
Litorânea	0,659	0,044	0,003	0,055	-0,088	0,702	0,003	0,748
Paranapanema I	0,882	0,022	0,001	0,029	-0,069	0,660	-0,030	0,887
Paranapanema II	0,899	0,017	0,000	0,022	-0,071	0,746	-0,082	0,845
Paranapanema III	0,881	0,024	0,001	0,027	-0,060	0,720	-0,054	0,993
Paranapanema IV	0,647	0,037	0,002	0,045	-0,058	0,754	-0,017	0,773
Paraná I	0,841	0,020	0,001	0,029	-0,104	0,668	0,021	0,601
Paraná II	0,890	0,025	0,001	0,032	-0,158	0,462	0,043	0,573
Paraná III	0,861	0,028	0,001	0,036	-0,136	0,509	0,082	0,552
Piquiri	0,734	0,018	0,001	0,024	-0,070	0,692	-0,009	0,559
Pirapó	0,765	0,037	0,002	0,049	-0,041	0,751	-0,057	0,949
Ribeira	0,514	0,026	0,001	0,034	-0,043	0,988	-0,046	0,666
Tibagi	0,593	0,023	0,001	0,030	0,002	0,983	-0,070	0,846

The Cinzas, Paranapanema I, II, III, Paraná I, II, III, Piquiri, and Pirapó watersheds exhibited the highest R^2 values, ranging from 0.73 to 0.89, indicating a consistent model fit for these areas. In these watersheds, validation metrics showed low MAE, MSE, and RMSE values, all below 0.049, reinforcing the model's strong predictive capability. The Ivaí, Coastal, and Paranapanema IV watersheds presented intermediate R^2 values (0.64–0.67), indicating that the model captured a substantial portion of the variability, although approximately 33% to 36% of the variability remained unexplained. In these cases, MAE, MSE, and RMSE values ranged from 0.001 to 0.055, suggesting moderate but stable performance. A similar pattern was observed for the Itararé (R^2 = 0.57), Ribeira (R^2 = 0.51), and Tibagi (R^2 = 0.59) watersheds. The Iguaçu basin recorded the lowest R^2 value (0.46), indicating a larger discrepancy between observed and predicted values and a lower model fit compared to the other watersheds. However, MAE (0.037), MSE (0.002), and RMSE (0.045) values were low in the Iguaçu basin, indicating that the model did not produce significant absolute errors.

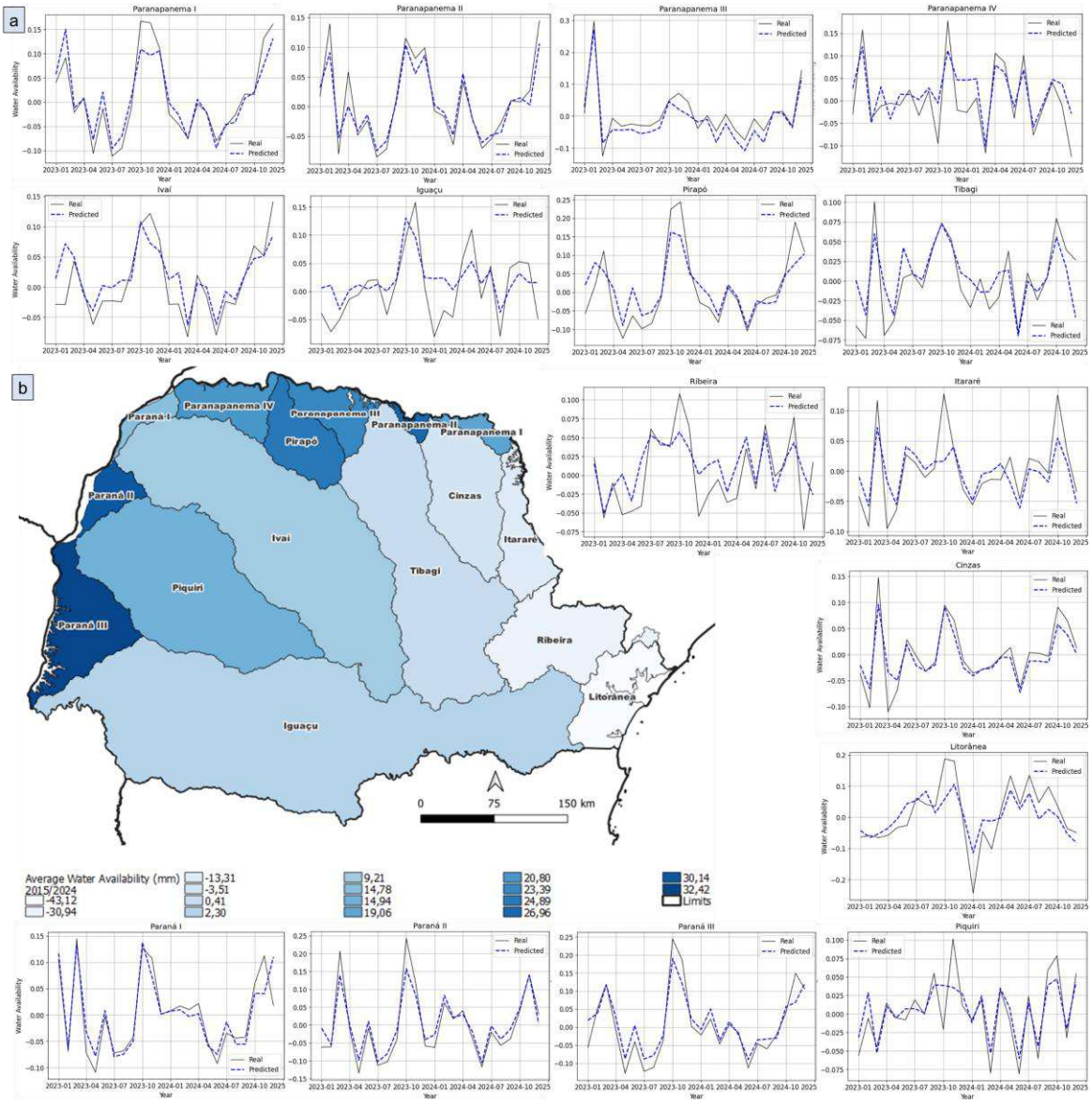


Figure 11 – Time series of machine learning predictions (a) and spatial distribution of mean water availability values by hydrographic basin (b).

Precipitation projections, evaluated under two greenhouse gas emission scenarios, SSP2-4.5 (intermediate) and SSP5-8.5 (pessimistic), indicated a general decreasing trend in precipitation, particularly under the intermediate scenario (Table 4). Under the SSP2-4.5 scenario for the period 2026–2035, only the Tibagi basin did not exhibit a negative trend in accumulated precipitation (+0.21 mm). The most pronounced reductions occurred in the Paraná II (-18.96 mm), Paraná III (-16.29 mm), and Paraná I (-12.46 mm) watersheds, all located in the far western sector of the state, as well as in the Coastal basin (-10.54 mm) (Figure 12b). Under the SSP5-8.5 scenario (pessimistic), although some watersheds showed reductions in precipitation, ranging from -9.85 to -1.10 mm, positive trends were observed in other regions. Notably, the Paraná III (+9.79 mm), Iguaçu (+6.53 mm), Paraná II (+5.19 mm), Paraná I (+2.49 mm), and Coastal (+0.36 mm) watersheds exhibited increases in projected precipitation (Figure 12c).

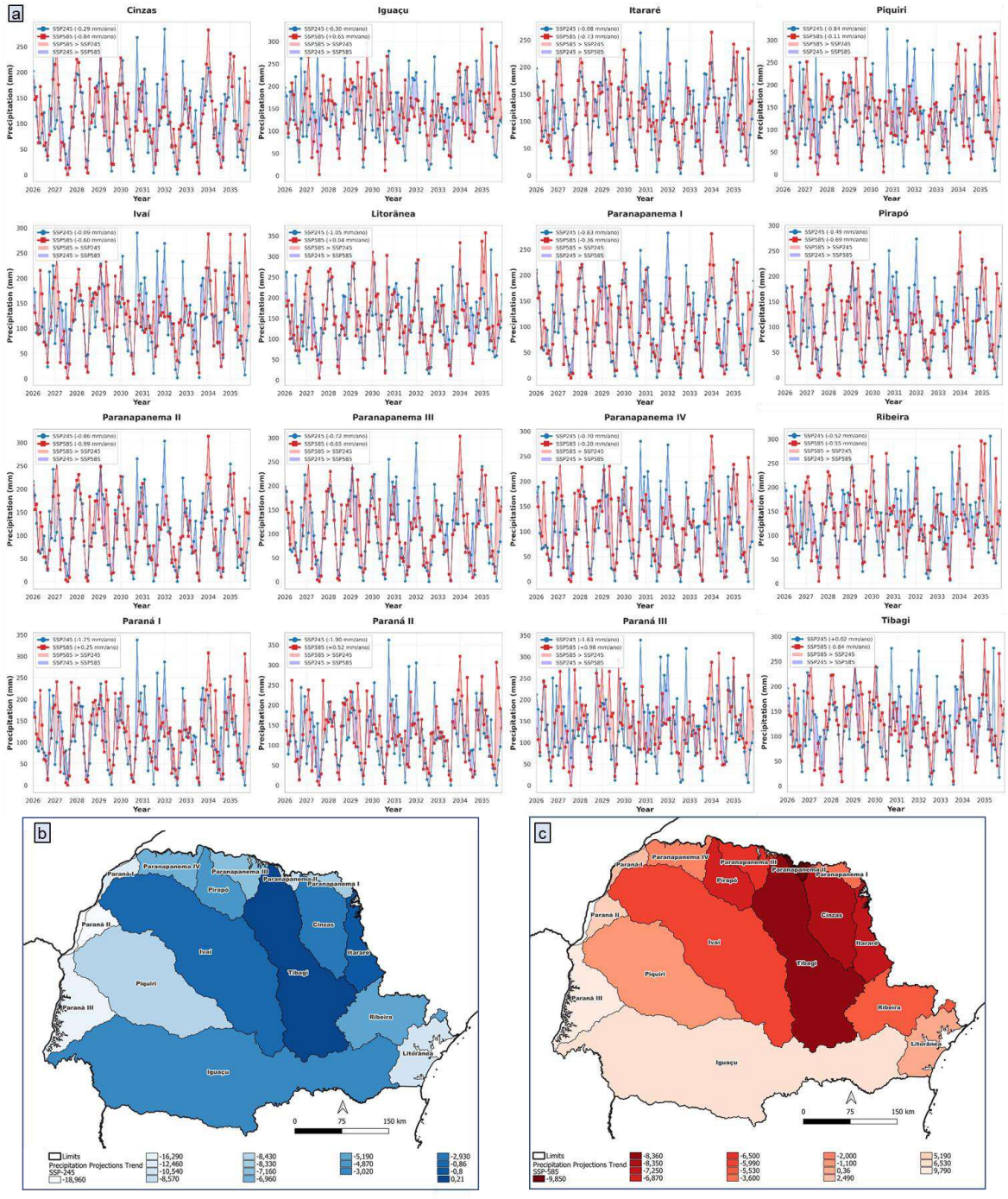


Figure 12 – Time series of future precipitation scenarios (a) and spatial distribution of the intermediate (b) and pessimistic (c) scenarios by hydrographic basin.

4. Discussion

4.1. Aquaculture Expansion and Environmental Challenges

Aquaculture has emerged as a key component for food security, representing one of the fastest-growing food production sectors globally (FAO, 2024). In Paraná, this trend is manifested in an intense and concentrated process of spatial and productive expansion, particularly in the Paraná III and Piquiri watersheds, which have become the state's primary hubs for the activity, followed by the Iguaçu basin, albeit at a lower intensity. The spatiotemporal analysis showing a concentration of aquaculture farms in areas with environmental and structural conditions favorable to

production intensification. This dynamic highlights the importance of understanding spatial patterns of aquaculture at different scales to support territorial planning and food security in emerging countries (Xia, Guo, & Chen, 2020).

RF algorithm demonstrated high accuracy, ranging from 0.89 to 0.98, confirming the efficiency of automated mapping methods and the potential of integrating high-resolution data with machine learning algorithms (Deeks et al., 2024; Liu et al., 2024; Zhao et al., 2025b). These results are consistent with recent studies showing the capacity of such techniques to extract aquaculture features with high spatial detail (Dong et al., 2024; Liang et al., 2024; Qin et al., 2025). Accordingly, Paraná's aquaculture sector can benefit from the implementation of targeted policies and actions aligned with regional characteristics (Diniz et al., 2021) and basin water availability, ensuring sustainable development and efficient management of the aquaculture industry (Tian et al., 2022).

Although results indicate consistent production growth, reaching 250,000 t in 2024 and, in some cases, growth rates exceeding 600%, as observed in the Pirapó, Paraná II, and Ivaí watersheds, this expansion occurred alongside a negative streamflow trend in all hydrographic watersheds in the state. Such patterns may be linked to continental-scale hydrological changes influenced by land use and land cover changes, increased agricultural water withdrawals, and climatic variability (Cremon et al., 2025). These findings align with international studies indicating that over 90% of global aquaculture production is vulnerable to human-induced environmental changes (Cao et al., 2023), particularly under shifts in thermal and hydrological regimes (Cortes et al., 2025).

This scenario may contribute to increased volatility in enterprise growth and production rates, as observed in Paraná, with periods of strong expansion (400%) followed by contraction (-200%). In the Paraná III and Piquiri watersheds, which are major aquaculture producers with well-established production infrastructure and cooperative networks among key supply chain actors (Brenzan & Feiden, 2022; Feiden et al., 2018), a declining streamflow trend was observed (-16.7 to -33.9 $m^3 s^{-1} yr^{-1}$). Similar situations have been reported in other Latin American contexts, such as Chile (Boisier et al., 2025), where increasing water scarcity is directly linked to land use changes and the expansion of agricultural and aquaculture activities, reflecting patterns comparable to those in Paraná. In response, state agencies implemented water use control and restriction policies between 2022 and 2025, declaring critical areas for water withdrawal and management (IAT, 2025a). Without planned interventions, continued intensive expansion may increase water competition at the state level, exacerbate pollution problems, and lead to production declines related to pathogens in areas with uncontrolled growth (Naylor et al., 2021), as has already been observed in Paraná III sub-watersheds, where high rates of pond eutrophication occur (Morsoleto et al., 2022).

Temporal meteorological analysis (2015–2024) revealed a general reduction in precipitation across the state. Although broader spatiotemporal hydrometeorological analyses (ANA, 2024; Tavares et al., 2023) have indicated increasing atmospheric moisture, extreme precipitation events are also intensifying in southern Brazil and the Paraná and South Atlantic sub-watersheds. Observed evapotranspiration values for Paraná corroborate the increasing trend reported in other regions of the country (Rossi et al., 2024), reflecting higher evaporative demand and consequent pressure on water resources, especially in areas with already critical water balances. Combined with significant surface runoff (up to 317.57 mm), these factors directly reduce water availability, increasing water vulnerability for small-scale producers (Rocha et al., 2021). Additional studies indicate that evaporation from reservoirs and aquaculture ponds can significantly affect intensive production systems, exacerbating water stress for rural producers (Yusoff et al., 2024). Our findings also revealed a positive trend in land surface temperature, ranging from 0.03 to 0.09 °C yr^{-1} in most watersheds, affecting the thermal conditions of excavated ponds and aligning with projections of rising temperatures in southern Brazil (Nóia-Júnior, Christo, & Pezzopane, 2025).

Given these patterns, public policies and technical assistance must consider the territorial diversity of aquaculture (Pacheco et al., 2025; Valenti et al., 2021). Clusters 1 and 2, which include most watersheds, show weaker

links between production and growth, indicating technical or water constraints that limit productivity gains. This highlights the need for targeted policies, technical support, cooperativism, and supply chain integration to strengthen these areas (Welter et al., 2021; FAO, 2024; Kyvelou, Ierapetritis, & Chiotinis, 2023). An integrated approach emphasizes institutional strengthening, decentralized management, and local engagement to enhance resilience, especially in less consolidated regions. In contrast, cluster 3 (Iguaçu, Piquiri, and Paraná III) is strongly associated with production variables, reflecting better infrastructure, market access, and incentives (Feiden et al., 2018). This is reinforced by strong positive correlations (>0.90) between production and spatial expansion, highlighting the need for planning to sustain growth (Naylor et al., 2021).

4.2. Water Availability, Prediction, and Future Precipitation

The Litorânea, Ribeira, Cinzas, and Itararé watersheds, located in the eastern sector of the state, showed the highest frequency of water deficit periods, particularly between 2018 and 2024. In contrast, watersheds in the western sector of the state exhibited a higher frequency of positive water availability values, with an increasing trend (0.08 to 4.67 mm yr^{-1}), as these areas correspond to regions with higher annual precipitation rates (Wrege et al., 2016). These findings emphasize that regional hydrological dynamics directly influence aquaculture, highlighting the importance of integrated water resource management in productive expansion strategies (Dolores-Salinas & Miret-Pastor, 2024; Ribeiro & Filho, 2025) to strengthen both water and institutional resilience in Paraná's aquaculture sector. This is particularly relevant in watersheds where aquaculture is already consolidated (Feiden et al., 2018), representing a risk factor for maintaining statewide production. Our findings suggest that this risk may increase due to projected precipitation reductions up to 2035 under the SSP2-4.5 scenario (Tebaldi et al., 2021; Thrasher et al., 2022), especially in the Paraná III and Piquiri watersheds. Consequently, as water deficits intensify under the SSP2-4.5 scenario, these watersheds are expected to experience an increase in local and regional extreme events (Clarke et al., 2024; Schmoeller & Limberger, 2023).

Our model demonstrated strong predictive performance, particularly in watersheds with lower climatic variability, achieving $R^2 > 0.80$. This performance, even though the training dataset covered a relatively short temporal period, indicates that the predictions are consistent (Mohamad Deros, Naim, & Din, 2025), given the RF algorithm's high predictive capability (Gao et al., 2025; Mohammadi, Pishgar, & Aguilera, 2025). It is noteworthy that in larger watersheds, which often present greater climatic and topographic variability (Carpenedo, Bonfim, & Limberger, 2024; Santos, Allen, & Nascimento, 2025; Schmoeller & Limberger, 2023), such as the Iguaçu basin, model performance was lower.

5. Conclusions

The study revealed a challenging medium-term scenario for the expansion of excavated pond aquaculture in Paraná, with strong concentration in the western sector of the state. This pattern of spatial concentration in areas of productive intensification may significantly increase pressure on water resources and elevate the risk of water use conflicts, especially under uncertain climatic scenarios that could reduce water availability or generate scenarios of decreased (SSP2-4.5) and increased precipitation (SSP5-8.5), along with extreme events in the primary production hubs.

Multivariate analysis (PCA and clustering) identified two main spatial patterns: watersheds with negative correlations between hydrometeorological variables and fish production, associated with frequent water deficits (clusters 1 and 2), and more productive watersheds (Iguaçu, Piquiri, and Paraná III) with positive correlations between production and territorial expansion. Concentrated in the western region, these areas combine larger size, more farms, higher output,

and better infrastructure, supported by favorable water availability. The results emphasize the need for integrated state-level planning tailored to basin-specific characteristics, promoting balanced aquaculture expansion and supporting regions with spatial growth but limited gains in production value.

Consequently, the proposed machine learning–based water availability prediction model, with good predictive capability ($R^2 > 0.80$), can provide forecasts at the scale of hydrographic watersheds, supporting the formulation of more targeted public policies in the medium term. Finally, it is recommended that future studies refine the model by incorporating long-term temporal data and climate uncertainty scenarios, particularly when applied to large-scale hydrographic watersheds.

Competing interests

Financial support was received from Araucária Foundation for Scientific and Tecnological Development of Paraná State and the Secretariat for Science, Technology, and Higher Education (Fundação Araucária e a Secretaria de Ciência, Tecnologia e Ensino Superior - SETI) of the State of Paraná - Covenant Agreement No. 215/2023, Biopark Education (Biopark Educação) and Donaduzzi family.

Funding statement

Financial support was received from Araucária Foundation for Scientific and Tecnological Development of Paraná State and the Secretariat for Science, Technology, and Higher Education (Fundação Araucária e a Secretaria de Ciência, Tecnologia e Ensino Superior - SETI) of the State of Paraná - Covenant Agreement No. 215/2023, Biopark Education (Biopark Educação) and Donaduzzi family.

References

Aghakouchak, A., Feldman, D., Hoerling, M., Huxman, T., Lund, J., 2015. Remote sensing of drought: Progress, challenges and opportunities. Rev. Geophys. 53 (2), 452–480. https://doi.org/10.1002/2014RG000456

Akiba, T., Sano, S., Yanase, T., Ohta, T., Koyama, M., 2019. Optuna: A next-generation hyperparameter optimization framework. Proc. 25th ACM SIGKDD Int. Conf. Knowl. Discov. Data Min. https://doi.org/10.1145/3292500.3330701

Almeida, C.R., Teodoro, A.C., Gonçalves, A., 2023. Time-series analyses of land surface temperature changes with Google Earth Engine in a mountainous region. Heliyon 9 (8), e18872. https://doi.org/10.1016/j.heliyon.2023.e18872

Alvares, C.A., Stape, J.L., Sentelhas, P.C., Gonçalves, J.L.M., Sparovek, G., 2013. Köppen's climate classification map for Brazil. Meteorol. Z. 22 (6), 711–728. https://doi.org/10.1127/0941-2948/2013/0507

Althoff, D., Rodrigues, L.N., Silva, D.D., 2021. Assessment of water availability vulnerability in the Cerrado. Appl. Water Sci. 11 (11), 178. https://doi.org/10.1007/s13201-021-01502-1

Amani, M., Ghorbanian, A., Ahmadi, S.A., Kakooei, M., Moghimi, A., Mirmazloumi, S.M., Alizadeh Moghaddam, S.H., Mahdavi, S., Ghahremanloo, M., Parsian, S., Wu, Q., Brisco, B., 2020. Google Earth Engine cloud computing platform for remote sensing big data applications: A comprehensive review. IEEE J. Sel. Top. Appl. Earth Obs. Remote Sens. 13, 5326–5350. https://doi.org/10.1109/JSTARS.2020.3021052

Amiri, M., Salem, A., Ghzal, M., 2022. Spatial-temporal water balance components estimation using integrated GIS-based WetSpass-M model in Moulouya Basin, Morocco. ISPRS Int. J. Geo-Inf. 11 (2), 123. https://doi.org/10.3390/ijgi11020123

Agência Nacional de Águas e Saneamento Básico (ANA), 2024. Impacto da mudança climática nos recursos hídricos no Brasil. ANA, Brasília.

Agência Nacional de Águas e Saneamento Básico (ANA), 2025. Metadados dos dados hidrológicos – Sistema de Informações Hidrológicas (Hidroweb). ANA, Brasília. Disponível em: https://www.snirh.gov.br/hidroweb/ (accessed 20 July 2025).

Associação Brasileira da Piscicultura (Peixe BR), 2025. Anuário brasileiro da piscicultura PEIXE BR 2025: O mapa da piscicultura brasileira. Peixe BR, Brasília.

Bao, Z., Zhang, J., Wang, G., Fu, G., He, R., Yan, X., Jin, J., Liu, Y., Zhang, A., 2019. The impact of climate variability and land use/cover change on the water balance in the Middle Yellow River Basin, China. J. Hydrol. 577, 123942. https://doi.org/10.1016/j.jhydrol.2019.123942

Barange, M., Bahri, T., Beveridge, M.C.M., Cochrane, K.L., Funge-Smith, S., Poulain, F., 2018. Impacts of climate change on fisheries and aquaculture: Synthesis of current knowledge, adaptation and mitigation options. FAO Fish. Aquac. Tech. Pap. 627.

Barbedo, R., Siqueira, V.A., Fan, F.M., Collischonn, W., 2022. Water storage variability across Brazil. Rev. Bras. Recur. Hídricos 27, e18. https://doi.org/10.1590/2318-0331.272220210156

Battisti, R., Sentelhas, P.C., Boote, K.J., Câmara, G.M.S., Farias, J.R.B., 2025. Assessing precipitation trends between 1960 and 2021 using multiple trend indexes in Goiás State and Federal District, Brazil. Int. J. Climatol. https://doi.org/10.1002/joc.XXXX

Béné, C., Barange, M., Subasinghe, R., Pinstrup-Andersen, P., Merino, G., Hemre, G.I., Williams, M., 2015. Feeding 9 billion by 2050 – Putting fish back on the menu. Food Secur. 7 (2), 261–274. https://doi.org/10.1007/s12571-015-0427-z

Bergmeir, C., Hyndman, R.J., Koo, B., 2017. A note on the validity of cross-validation for evaluating autoregressive time series prediction. Comput. Stat. Data Anal. 123, 70–83. https://doi.org/10.1016/j.csda.2018.01.003

Biazar, S.M., Mahdavi, S., Ghorbani, M.A., Kisi, O., 2025. Artificial intelligence in hydrology: Advancements in soil, water resource management, and sustainable development. Sustainability 17 (5), 2250. https://doi.org/10.3390/su17052250

Boisier, J.P., Alvarez-Garreton, C., Cordero, R.R., Damiani, A., Gallardo, L., Garreaud, R., Lambert, F., Ramallo, C., Rojas, M., Rondanelli, R., 2025. Increasing water stress in Chile revealed by novel datasets of water availability, land use and water use. Hydrol. Earth Syst. Sci. 29 (20), 5185–5212. https://doi.org/10.5194/hess-29-5185-2025

Breiman, L., 2001. Random forests. Mach. Learn. 45, 5–32. https://doi.org/10.1023/A:1010933404324

Brenzan, C.K.M., Feiden, A., 2022. A piscicultura como atividade propulsora do desenvolvimento da mesorregião oeste do Paraná. Res. Soc. Dev. 11 (14), eXXXX. https://doi.org/10.33448/rsd-v11i14.XXXX

Campos-Taberner, M., García-Haro, F.J., Camps-Valls, G., Grau-Muedra, G., Nutini, F., Crema, A., Boschetti, M., 2018. Global estimation of biophysical variables from Google Earth Engine platform. Remote Sens. 10 (8), 1167. https://doi.org/10.3390/rs10081167

Cao, L., Naylor, R., Henriksson, P.J.G., Leadbitter, D., Metian, M., Troell, M., Zhang, W., 2023. Vulnerability of blue foods to human-induced environmental change. Nat. Sustain. 6 (10), 1186–1198. https://doi.org/10.1038/s41893-023-01169-2

Carpenedo, C.B., Bonfim, A.L.S., Limberger, L., 2024. Variabilidade climática e circulação atmosférica anômala durante os extremos chuvosos em Curitiba-PR. Rev. Bras. Climatol. 34, 242–264.

Chernykh, D., Kalashnikov, A., Zhumabayev, A., Yegizbayeva, A., 2025. Spatiotemporal analysis of soil moisture variability and precipitation response across soil texture classes in East Kazakhstan. Land 14 (6), 1136. https://doi.org/10.3390/land14061136

Ciampittiello, M., Marchetto, A., Boggero, A., 2024. Water resources management under climate change: A review. Sustainability 16, XXXX. https://doi.org/10.3390/suXXXX

Clarke, B., Otto, F.E.L., Stuart-Smith, R., Harrington, L., 2024. Climate change, El Niño and infrastructure failures behind massive floods in southern Brazil. KNMI Rep., 1–56.

Cleveland, R.B., Cleveland, W.S., McRae, J.E., Terpenning, I., 1990. STL: A seasonal-trend decomposition procedure based on Loess. J. Off. Stat. 6 (1), 3–73.

Cortes, J.R., Ferreira, J.G., Bricker, S., 2025. Climate-smart aquaculture: Innovations and challenges in mitigating climate change impacts on fisheries and coastal agriculture. Aquac. Fish. https://doi.org/10.1016/j.aaf.2025.XXXX

Cremon, É.H., Siqueira, V.A., Fan, F.M., Collischonn, W., 2025. Hydrological shifts in the Cerrado's largest free-flowing river under land use and climate pressure. J. South Am. Earth Sci. 105615. https://doi.org/10.1016/j.jsames.2025.105615

Cunico, C., Prim, D., 2018. Zoneamento ecológico-econômico do estado do Paraná. Instituto de Terras, Cartografia e Geologia, Curitiba.

Dahan, K.S., Adjakpa, J.B., Yao, B.K., 2023. Environmental and climatic changes and wildfire spread in Ghana using remote sensing and machine learning (GEE). Int. J. Digit. Earth 16 (1), 1300–1331. https://doi.org/10.1080/17538947.2023.219XXXX

Dapieve, D.R., Novo, Y.C.C., Feiden, A., 2023. Use of geotechnologies for aquaculture site selection: Suitability factors and constraints for production in ground-excavated ponds. Lat. Am. J. Aquat. Res. 51 (2), 160–194. https://doi.org/10.3856/vol51-issue2-fulltext-XXXXX

Deeks, E., Smith, G., Jones, T., Williams, R., 2024. Seagrass mapping of north-eastern Brazil using Google Earth Engine and Sentinel-2 imagery. Environ. Sustain. Indic. 24, XXXX. https://doi.org/10.1016/j.indic.2024.XXXX

Diniz, C., Cortinhas, L., Rodrigues, J., Pereira, L., Luz, N., de Carvalho, A., Souza, C., 2021. A large-scale deep-learning approach for multi-temporal aqua and salt-culture mapping. Remote Sens. 13 (8), 1418. https://doi.org/10.3390/rs13081418

Dolores-Salinas, E., Miret-Pastor, L., 2024. Environmental certifications in Brazilian aquaculture. Aquac. Int. 32 (6), 8609–8630. https://doi.org/10.1007/s10499-024-XXXX

Dong, D., Zhang, Y., Li, X., Wang, J., 2024. Intelligent detection of marine offshore aquaculture with high-resolution optical remote sensing images. J. Mar. Sci. Eng. 12 (6), XXXX. https://doi.org/10.3390/jmse1206XXXX

Erekalo, K.T., Tesfaye, K., Alemu, D., 2024. Contribution of farming practices and technologies towards climate-smart agricultural outcomes in Europe. Smart Agric. Technol. 7, XXXX. https://doi.org/10.1016/j.atech.2024.XXXX

Et-taibi, B., Boulfoul, B., El Alami, R., 2024. Enhancing water management in smart agriculture: A cloud and IoT-based smart irrigation system. Results Eng. 22, XXXX. https://doi.org/10.1016/j.rineng.2024.XXXX

FAO, 2024. The state of world fisheries and aquaculture 2024 – Blue transformation in action. FAO, Rome. https://doi.org/10.4060/cc0461en

Farias, F., Silva, R., Souza, A., Gomes, H., 2023. Large-scale water balance modeling using remote sensing and weather data in northeastern Brazil. Remote Sens. Appl. Soc. Environ. 32, XXXX. https://doi.org/10.1016/j.rsase.2023.XXXX

Feiden, A., Ramos, M.J., Chidichima, A.C., 2018. A cadeia produtiva da tilápia no oeste do Paraná: formação de arranjo produtivo local. Redes 23 (2), 238–263.

Ferreira, F.L.V., Mello, C.R., Viola, M.R., 2023. Spatial–temporal variability of climatic water balance in Brazilian savannah watersheds. Water 15 (10), XXXX. https://doi.org/10.3390/w1510XXXX

Fong, C.R., Ayala, G.M., Jones, R., 2024. Downscaled climate change threats to U.S. freshwater finfish aquaculture. Sci. Total Environ. 957, XXXX. https://doi.org/10.1016/j.scitotenv.2024.XXXX

Funatsu, B.M., Silva Dias, M.A.F., Gan, M.A., 2025. Hydroclimatic extremes, land cover exposure, and vegetation responses in Brazil. Remote Sens. Appl. Soc. Environ. 101595. https://doi.org/10.1016/j.rsase.2025.101595

Funk, C., Peterson, P., Landsfeld, M., Pedreros, D., Verdin, J., Shukla, S., Husak, G., Rowland, J., Harrison, L., Hoell, A., Michaelsen, J., 2015. The climate hazards infrared precipitation with stations (CHIRPS). Sci. Data 2, 150066. https://doi.org/10.1038/sdata.2015.66

Gao, X., Zhang, Y., Liu, Z., Wang, H., 2025. Machine learning to evaluate climate change impacts on wheat yields in China. Agric. Water Manag. 317, XXXX. https://doi.org/10.1016/j.agwat.2025.XXXX

Garajeh, M.K., Malekmohammadi, B., Jafari, H., 2024. Monitoring climate change impacts on water resources using remote sensing and GEE. Sci. Rep. 14 (1), XXXX. https://doi.org/10.1038/s41598-024-XXXX

Gorelick, N., Hancher, M., Dixon, M., Ilyushchenko, S., Thau, D., Moore, R., 2017. Google Earth Engine: Planetary-scale geospatial analysis for everyone. Remote Sens. Environ. 202, 18–27. https://doi.org/10.1016/j.rse.2017.06.031

Greve, P., Gudmundsson, L., Seneviratne, S.I., 2018. Global assessment of water challenges under uncertainty. Nat. Sustain. 1, 486–494. https://doi.org/10.1038/s41893-018-0139-7

Guo, Q., Zhang, Y., Ma, Z., 2020. Spatiotemporal evolution of evapotranspiration in China after 1998. Water 12 (11), XXXX. https://doi.org/10.3390/w1211XXXX

Gupta, H.V., Kling, H., Yilmaz, K.K., Martinez, G.F., 2009. Decomposition of the mean squared error and NSE performance criteria. J. Hydrol. 377 (1–2), 80–91. https://doi.org/10.1016/j.jhydrol.2009.08.003

Han, J., Kamber, M., Pei, J., 2011. Data mining: Concepts and techniques. Morgan Kaufmann, Burlington.

He, M., Anderson, M., Gao, F., 2025. Protocols for water and environmental modeling using machine learning in California. Hydrology. https://doi.org/10.3390/hydrologyXXXX

Hyndman, R.J., Athanasopoulos, G., 2018. Forecasting: Principles and practice. OTexts, Melbourne.

IAT, 2025. Metadados de séries históricas de qualidade da água e vazão. Instituto Água e Terra, Curitiba.

IAT, s.d. Áreas críticas quanto ao uso de recursos hídricos. Instituto Água e Terra, Curitiba.

IBGE, 2024. Pesquisa da Pecuária Municipal 2024. Instituto Brasileiro de Geografia e Estatística, Rio de Janeiro.

Ji, P., Wang, X., Liu, Y., Zhang, H., 2025. Projecting future wetland dynamics under climate change and land use pressure. Remote Sens. 17 (6), XXXX. https://doi.org/10.3390/rs1706XXXX

Kanja, K., Mutanga, O., Odindi, J., 2025. Mapping tropical dry Miombo woodlands using Sentinel imagery and machine learning. Remote Sens. Appl. Soc. Environ. 101615. https://doi.org/10.1016/j.rsase.2025.101615

Kumar, L., Mutanga, O., 2018. Google Earth Engine applications since inception: Usage, trends, and potential. Remote Sens. 10 (10), 1509. https://doi.org/10.3390/rs10101509

Kundu, S., Khare, D., Mondal, A., 2017. Impacts of climate and land use changes on water balance. Ecol. Eng. 105, 42–57. https://doi.org/10.1016/j.ecoleng.2017.04.018

Kyvelou, S.S., Ierapetritis, D.G., Chiotinis, M., 2023. Fisheries co-management and the blue economy. Sustainability 15 (10), XXXX. https://doi.org/10.3390/su1510XXXX

Łągiewska, M., Bartold, M., 2025. Remote sensing and decision analysis to mitigate drought. Remote Sens. 17 (7), XXXX. https://doi.org/10.3390/rs1707XXXX

Laipelt, L., Kayser, R.H.B., Fleischmann, A.S., Ruhoff, A.L., Bastiaanssen, W.G.M., Erickson, T.A., Melton, F.S., 2021. Long-term evapotranspiration monitoring using SEBAL and GEE. ISPRS J. Photogramm. Remote Sens. 178, 81–96. https://doi.org/10.1016/j.isprsjprs.2021.05.018

Laipelt, L., Ruhoff, A.L., Kayser, R.H.B., 2024. Evapotranspiration changes under cropland expansion. Remote Sens. 16, 3404. https://doi.org/10.3390/rs16173404

Liang, Z., Chen, Y., Li, J., 2024. Extraction of aquaculture ponds using multispectral fusion. Remote Sens. 16, XXXX. https://doi.org/10.3390/rs16XXXX

Liu, C., Li, X., Zhang, Y., Wang, J., 2024. Mapping aquaculture ponds using Sentinel-1 imagery. Aquaculture 581, XXXX. https://doi.org/10.1016/j.aquaculture.2024.XXXX

Lopes, T.R., Mello, C.R., Viola, M.R., 2021. Land use impacts on water balance in the Amazon. J. South Am. Earth Sci. 108, XXXX. https://doi.org/10.1016/j.jsames.2021.XXXX

Loureiro, B.R., Feiden, A., Novo, Y.C.C., 2024. Fish farming environmental suitability scenarios. Bol. Inst. Pesca 50, XXXX. https://doi.org/10.20950/1678-2305/bip.2024.50.XXXX

Mello, C.R., Viola, M.R., Beskow, S., Norton, L.D., 2019. Water balance in a neotropical forest catchment. Catena 173, 9–21. https://doi.org/10.1016/j.catena.2018.10.002

Melnyk, O., Brunn, A., 2025. Water regime trends using Sentinel-2 indices. Remote Sens. 17 (14), 2363. https://doi.org/10.3390/rs17142363

Mohamad Deros, S.N., Naim, M.R., Din, N.M., 2025. Explainable AI for land subsidence prediction. Total Environ. Adv. 15, XXXX. https://doi.org/10.1016/j.tead.2025.XXXX

Mohammadi, A., Pishgar, E., Aguilera, J., 2025. Machine learning for asthma risk prediction. ISPRS Int. J. Geo-Inf. 14 (3), XXXX. https://doi.org/10.3390/ijgi1403XXXX

Morsoleto, F.M.S., Feiden, A., Novo, Y.C.C., 2022. GIS for assessing aquaculture ponds. Bol. Inst. Pesca 48, e695.

NASA, 2023. Moderate Resolution Imaging Spectroradiometer (MODIS). NASA.

Nascimento, R.S., Borges, V.P., Diniz Melo, D.C., 2023. Climate change impacts on water availability. Rev. Ceres 70 (3), XXXX. https://doi.org/10.1590/0034-737X202370030XXX

Naylor, R.L., Hardy, R.W., Buschmann, A.H., Bush, S.R., Cao, L., Klinger, D.H., Little, D.C., Lubchenco, J., Shumway, S.E., Troell, M., 2021. A 20-year review of global aquaculture. Nature 591, 551–563. https://doi.org/10.1038/s41586-021-03308-6

Nóia-Júnior, R.S., Christo, B.F., Pezzopane, J.E.M., 2025. Extreme weather and agricultural collapse in southern Brazil. Next Res. 2 (2), 100217. https://doi.org/10.1016/j.nexres.2025.100217

Novo, Y.C.C., Feiden, A., Dapieve, D.R., 2022. Mapping aquaculture units in Paraná. RA'E GA 54, 103–108.

Novruzova, A., 2021. Climate change impact on water resources. Teka Polit. Sci. Int. Relat. 16 (2), 23–35.

Ottinger, M., Clauss, K., Kuenzer, C., 2018. Aquaculture production estimation using EO data. Remote Sens. 10 (7), 1076. https://doi.org/10.3390/rs10071076

Ottinger, M., Kuenzer, C., Liu, G., 2022. Mapping aquaculture ponds with Sentinel data. Remote Sens. 14 (1), XXXX. https://doi.org/10.3390/rs1401XXXX

Pacheco, F.S., Naylor, R., Boyd, C., 2025. Towards sustainable aquaculture in the Amazon. Nat. Sustain. https://doi.org/10.1038/s41893-025-XXXX

Parra-López, C., De Haro-Giménez, T., Sayadi, S., 2025. Digital technologies for water management in agriculture. Agric. Water Manag. https://doi.org/10.1016/j.agwat.2025.XXXX

Passos, F.O., Mello, C.R., Viola, M.R., 2025. Climate change and hydropower inflows in Brazil. Climate 13 (7), 140. https://doi.org/10.3390/cli13070140

Pedregosa, F., Varoquaux, G., Gramfort, A., Michel, V., Thirion, B., Grisel, O., Blondel, M., Prettenhofer, P., Weiss, R., Dubourg, V., Vanderplas, J., Passos, A., Cournapeau, D., Brucher, M., Perrot, M., Duchesnay, É., 2011. Scikit-learn: Machine learning in Python. J. Mach. Learn. Res. 12, 2825–2830.

Pérez-Cutillas, P., Zema, D.A., Lucas-Borja, M.E., 2023. Google Earth Engine: A systematic review. Remote Sens. Appl. Soc. Environ. https://doi.org/10.1016/j.rsase.2023.XXXX

Pérez-Cutillas, P., Salhi, A., 2024. Hydroclimatic projections in Morocco. J. Environ. Manag. 371, XXXX. https://doi.org/10.1016/j.jenvman.2024.XXXX

Pillar, V.D., Overbeck, G.E., 2024. Climate disaster in southern Brazil. Science 385, 1–2. https://doi.org/10.1126/science.XXXX

Planet Team, 2017. Planet application program interface: In space for life on Earth. Planet Labs, San Francisco.

QGIS Development Team, 2024. QGIS Geographic Information System. Open Source Geospatial Foundation. (Version 3.28.2).

Qin, W., Li, X., Zhang, Y., 2025. Deep learning extraction of aquaculture ponds. Sustainability 17 (16), XXXX. https://doi.org/10.3390/su1716XXXX

Rajandran, A., et al., 2022. Review of Google Earth Engine in aquaculture mapping. IOP Conf. Ser.

Ribeiro, V.S., Pedroza Filho, M.X., 2025. Institutional environment of Brazilian tilapia production. Rev. Econ. Sociol. Rural 63.

Rocha, N.S., Mello, C.R., Viola, M.R., 2021. Climate change impacts on hydric balance. Acta Geophys. 69 (4), 1427–1445.

Rossi, J.B., Mello, C.R., Viola, M.R., 2024. Evaporation in Brazilian reservoirs. J. South Am. Earth Sci. 140.

Santos, L.O., Allen, J.T., Nascimento, E.L., 2025. Severe storm trends in South America. Weather Clim. Extrem. 50.

Sapitang, M., et al., 2024. AI-GIS integration in water management. Remote Sens. Appl. Soc. Environ.

Schmoeller, A.M.P., Limberger, L., 2023. Climate change patterns in Paraná. Rev. Bras. Geogr. Física 16 (4), 1697–1713.

Serrão, E.A.O., et al., 2020. Land use change and hydropower in the Amazon. Sci. Total Environ. 744.

Silva, B.A., Ummus, M.E., Hayakawa, E.H., Trombini, M., 2024. Mapping aquaculture in Brazil using GEE. Remote Sens. Appl. Soc. Environ.

Silva, B.A., et al., 2021. Geomorphic evolution of the Basalt Plateau. J. South Am. Earth Sci. 110. https://doi.org/10.1016/j.jsames.2021.103351

Silva, C.O.F., Teixeira, A.H.C., Manzione, R.L., 2019. agriwater: R package for evapotranspiration modelling. Environ. Model. Softw. 120.

Silva, R.M., Lopes, A.G., Santos, C.A.G., 2023. Deforestation and rainfall variability in Amazon. J. Environ. Manag. 326.

Siyal, A.W., Gerbens-Leenes, P.W., Vaca-Jiménez, S.D., 2023. Freshwater competition among sectors. Water Resour. Ind. 29.

Souza, C.M., Shimbo, J.Z., Rosa, M.R., Parente, L.L., Alencar, A.A., Rudorff, B.F.T., Hasenack, H., Matsumoto, M., Ferreira, L.G., Souza-Filho, P.W.M., Oliveira, S.W., Rocha, W.F., Fonseca, A.V., Marques, C.B., Diniz, C.G., Costa, D., Monteiro, D., Rosa, E.R., Vélez-Martin, E., Weber, E.J., Lenti, F.E.B., Paternost, F.F., Pareyn, F.G.C., Siqueira, J.V., Viera, J.L., Neto, L.C.F., Saraiva, M.M., Sales, M.H., Salgado, M.P.G., Vasconcelos, R., Galano, S., Mesquita, V.V., Azevedo, T., 2020. Reconstructing land use changes in Brazil. Remote Sens. 12 (17), 2735. https://doi.org/10.3390/rs12172735

Sun, W., Li, X., Zhang, Y., 2024. Coastal aquaculture mapping in China. Int. J. Digit. Earth 17 (1).

Tanuja, Kumar, R., 2025. Climatic shifts in the Beas Basin. Sci. Total Environ. 984.

Tavares, P.S., Mello, C.R., Viola, M.R., 2023. Water balance under warming scenarios. Reg. Environ. Change 23.

Tebaldi, C., Debeire, K., Eyring, V., Fischer, E., Fyfe, J., Friedlingstein, P., Knutti, R., Lowe, J., O'Neill, B., Sanderson, B., van Vuuren, D., Riahi, K., 2021. CMIP6 climate projections. Earth Syst. Dyn. 12, 253–293. https://doi.org/10.5194/esd-12-253-2021

Thrasher, B., Maurer, E.P., McKellar, C., Duffy, P.B., 2022. NASA downscaled climate projections CMIP6. Sci. Data 9. https://doi.org/10.1038/s41597-022-01393-4

Tian, P., Li, X., Zhang, Y., 2022. Mapping aquaculture ponds using SAR imagery. Remote Sens. 14 (21).

Uchôa, J.G.S.M., et al., 2024. Streamflow leakage across Brazil. Nat. Commun. 15.

Valenti, W.C., Barros, H.P., Moraes-Valenti, P., Bueno, G.W., Cavalli, R.O., 2021. Aquaculture in Brazil: Past, present and future. Aquac. Rep. 19. https://doi.org/10.1016/j.aqrep.2021.100611

Vallino, E., Ridolfi, L., Laio, F., 2020. Economic water scarcity in agriculture. Environ. Sci. Policy 114, 73–85. https://doi.org/10.1016/j.envsci.2020.08.015

Velastegui-Montoya, A., Montalván-Burbano, N., Carrión-Mero, P., Morante-Carballo, F., & Herrera-Franco, G., 2023. Google Earth Engine: A global analysis and future trends. *Remote Sensing* 15(14). https://doi.org/10.3390/rs15143654

Vizzari, M., Hilal, M., Sigura, M., Antognelli, S., & Fiore, F., 2025. Urban greenery mapping using object-based classification and multi-sensor data fusion in Google Earth Engine. *Urban Forestry and Urban Greening* 105. https://doi.org/10.1016/j.ufug.2025.128279

Wang, D., Zhang, Y., Liu, X., Chen, Y., & Li, Z., 2024. Identify and map coastal aquaculture ponds and their drainage and impoundment dynamics. *International Journal of Applied Earth Observation and Geoinformation* 134. https://doi.org/10.1016/j.jag.2024.103930

Wang, M., Cui, Y., Li, X., Liu, Y., & Zhang, H., 2023. Interannual changes of coastal aquaculture ponds in China at 10-m spatial resolution during 2016–2021. *Remote Sensing of Environment* 284. https://doi.org/10.1016/j.rse.2022.113331

Wang, Y., & Razmjooy, S., 2024. Prediction of drought hydrological and water scarcity based on optimal artificial intelligence by developing a metaheuristic optimization algorithm. *Physics and Chemistry of the Earth* 135. https://doi.org/10.1016/j.pce.2024.103567

Weitzman, J., Filgueira, R., & Grant, J., 2021. Development of best practices for more holistic assessments of carrying capacity of aquaculture. Journal of Environmental Management 287. https://doi.org/10.1016/j.jenvman.2021.112332

Welter, E.C., Costa, M.S., Rocha, J.R., & Hoshino, E., 2021. A piscicultura como atividade agropecuária propulsora do desenvolvimento local e regional: O caso do município de Maripá/PR. Research, Society and Development 10(10), 1–10. https://doi.org/10.33448/rsd-v10i10.18874

WMO (World Meteorological Organization), 2023. The Global Climate 2011–2020: A decade of accelerating climate change. Geneva. https://doi.org/10.25607/OBP-3215

Wrege, M.S., Steinmetz, S., Reisser Júnior, C., & Almeida, I.R., 2016. Regiões com similaridade de comportamento hídrico no sul do Brasil. Ra'e Ga – O Espaço Geográfico em Análise 38, 365–384. https://doi.org/10.5380/raega.v38i0.43678

Xia, Z., Guo, X., & Chen, R., 2020. Automatic extraction of aquaculture ponds based on Google *Earth Engine.* Ocean and Coastal Management 198. https://doi.org/10.1016/j.ocecoaman.2020.105348

Yu, Z., Liu, Y., Wang, X., Zhang, Y., & Li, J., 2025. Inferring water quality in the Songhua River Basin using Random Forest regression based on satellite imagery and geoinformation. Hydrology 12(3). https://doi.org/10.3390/hydrology12030045

Yusoff, F.M., Boyd, C.E., Badiola, M., & Verdegem, M.C.J., 2024. Water quality management in aquaculture. Cambridge Prisms: Water 2. https://doi.org/10.1017/wat.2024.6

Yvoz, S., Ceglar, A., van der Velde, M., & Toreti, A., 2025. Assessing crop water deficiency for regional adaptation to climate change. Agricultural Water Management 314. https://doi.org/10.1016/j.agwat.2025.108969

Zhao, C., Li, J., Wang, Q., Zhang, Y., & Liu, X., 2025a. Evaluating spectral indices for water extraction: Limitations and contextual usage recommendations. International Journal of Applied Earth Observation and Geoinformation 139. https://doi.org/10.1016/j.jag.2025.104105

Zhao, Y., Lu, Z., & Wei, Y., 2019. An assessment of global precipitation and evapotranspiration products for regional applications. Remote Sensing 11(9). https://doi.org/10.3390/rs11091057

Zhao, Y., Chen, X., Wang, L., Li, Z., & Sun, H., 2025b. Spatiotemporal trends and driving forces of pig production in China and the United States. Earth Critical Zone 100036. https://doi.org/10.1016/j.ecz.2025.100036